New Insights into the Recovery of Strategic and Critical Metals by Solvent Extraction

Jason Love, Manuel Miguirditchian, A. Chagnes

▶ **To cite this version:**

Jason Love, Manuel Miguirditchian, A. Chagnes. New Insights into the Recovery of Strategic and Critical Metals by Solvent Extraction. Bruce A Moyer. Ion Exchange and Solvent Extraction, 23, CRC Press, pp.1-44, 2019, Changing the Landscape in Solvent Extraction, 9781315114378. hal-02265140

HAL Id: hal-02265140

https://hal.univ-lorraine.fr/hal-02265140

Submitted on 20 Aug 2019

HAL is a multi-disciplinary open access archive for the deposit and dissemination of scientific research documents, whether they are published or not. The documents may come from teaching and research institutions in France or abroad, or from public or private research centers.

L'archive ouverte pluridisciplinaire **HAL**, est destinée au dépôt et à la diffusion de documents scientifiques de niveau recherche, publiés ou non, émanant des établissements d'enseignement et de recherche français ou étrangers, des laboratoires publics ou privés.

New insights into the recovery of strategic and critical metals by solvent extraction: the effects of chemistry and the process on performance

Jason B. Love (ORCID 0000-0002-2956-258X)

EaStCHEM School of Chemistry, University of Edinburgh, Edinburgh EH9 3FJ (UK).

Manuel Miguirditchian (ORCID 0000-0002-7676-757X)

CEA, Alternative Energies and Atomic Energy Commission, Nuclear Energy Division, Research Department on Mining and Fuel Recycling Processes, Centre de Marcoule, F-30207 Bagnols sur Cèze (France).

Alexandre Chagnes (ORCID 0000-0002-4345-6812)

Université de Lorraine, CNRS, GeoRessources, F- 54000 Nancy, France.

Abstract

Solvent extraction is a mature technology for the recovery of metals from primary and secondary resources, though it is still evolving in its chemistry, processes, and equipment, sometimes in disruptive fashion. Solvent extraction processes can be conceived, developed, and optimized by playing both on the physicochemistry, the technologies, and the flowsheets. The physicochemistry of solvent extraction is complicated, as it involves two immiscible phases and an interfacial zone in which many chemical equilibria occur, while flowsheet design has to take into account economic and ecologic considerations besides an easy integration in the chain value. This chapter aims at showing how solvent extraction flowsheets can be developed by using an integrated view from the molecule to the process. First, this chapter introduces a rational approach based on the comprehension of the role of coordination chemistry and physicochemistry to design new extracting agents. This approach is illustrated by two case studies: the design of new extractants in nuclear processing and the design of new extractants for recycling processes. Second, this chapter shows how can solvent extraction processes be improved by using flowsheet design tools and how can a process developed from the molecule to the flowsheet with a particular attention to the treatment of e-wastes.

1. Introduction

The exploitation of nonthermal chemical separation processes would lower global energy use, emissions, and pollution and is particularly pertinent to the recovery of metals from their primary ores and secondary resources [1]. In principle, the separation of metals by hydrometallurgical processes such as solvent extraction (SX, Figure 1) can achieve these outcomes due to ambient-temperature operation and the maintenance of materials balance through reagent recycling [2]. However, significant challenges remain, not least with attaining high levels of separation between metals, but also with issues such as reagent stability, complexity, cost, safety, and recyclability [3, 4].

Insert Figure 1 here

Optimization of SX processes is one of these challenges in order to treat new unconventional primary and secondary resources, especially polymetallic and low-grade resources. Although the ease of contacting two liquid phases is one of the key advantages of SX, the physicochemistry involved is very complex due to the existence of associations at molecular and supramolecular levels, nonideality, and the presence of various reactions in the aqueous and organic phases as well as in the liquid-liquid interface, which governs the kinetics of extraction (Figure 2) [5].

Insert Figure 2 here

The performance of solvent extraction processes mainly relies on the properties of extractant molecules for the selectivity needed for increasingly challenging problems. Surprisingly, there are relatively few extracting agents available on the market, and these molecules were mostly found more than fifteen-twenty years ago in spite of great efforts in the literature to develop new ones. Industry representatives repeatedly cite the high costs of chemical development and long times for testing and regulatory approval of new reagents as impediments. Developing faster and better approaches to designing new extractants appears therefore of great importance toward building efficient, low-cost, and sustainable processes capable to extract metals from new complex resources. However, the design of new extracting agents

cannot be performed by considering only their chemical structures, because interactions involving extractants strongly influences extractant properties. The molecular environment around the extractant, including diluent, phase modifier, other extractant molecules, etc., must thus be first understood and then taken into account during extraction solvent design. For this goal, modelling tools such as DFT (Density Functional Theory), semi-empirical and QSPR (Quantitative Structure-Property Relationship) calculations are increasingly playing an important role [6-8]. Nevertheless, the degree of reliability of the predictions is still limited, and in the present state of the art, these techniques are likely more useful for optimization within a given family of extractants than to build *in silico* new reagents. The molecular modelling techniques provide binding energies between target metals and given ligands, as well as optimized chemical structures of the formed complexes. Thus, in principle, the information which can be deduced from the molecular modelling computations is richer than that provided by QSPR methods. Modelling tools are an asset to understand liquid-liquid extraction phenomena. The comprehension of the physicochemistry involved during liquid-liquid extraction is therefore particularly important to optimize solvent extraction processes. It paves the way of the development of simulation process tools which are of great importance for optimizing processes.

Likewise, the optimization of the flowsheets is another way to improve the performances of solvent extraction processes in terms of extraction efficiency and selectivity. The classical Mc Cabe Thiele approach is usually used to choose the number of contactors to implement in the process. Such an approach is only based on engineering process calculations. Undoubtedly, the development of new approaches combining the physicochemistry of extraction solvent and engineering process calculations would help the engineer to optimize its process while using a minimum of expensive experiments.

This chapter gives an overview on new insight into the recovery of strategic and critical metals by solvent extraction. Particular attention is paid to explaining how it is possible to improve existing processes by playing both on the chemistry and the flowsheet design.

2. Extractant design

2.1. The role of coordination chemistry and supramolecular chemistry on the design of new extractants

The development of new reagents for solvent extraction processes requires an understanding of the fundamental solution chemistry of metals and their compounds in both aqueous and organic phases. Ultimately, however, the thermodynamic stability of the metal compound in the organic phase must be greater than that in the aqueous phase for the equilibrium to favor extraction. These facets have been analyzed in terms of the mechanism of extraction, namely how the metal is transferred from the aqueous to organic phase, as a cation (M^{n+}), anion (MX_m^{n-}), or salt (MX_m) [9]. This analysis requires combinations of expertise in coordination and supramolecular chemistry in particular, along with a myriad of experimental and computational characterization methods, to gain a proper understanding of the solvent extraction process. This part of the chapter will provide an overview on the role of coordination and supramolecular chemistry on solvent extraction processes, and will highlight the different types of extraction, the compounds formed, their characterization, and the impact on the design of new reagents. In keeping with the classifications of extractants described above, new advances will be described according to the metal species that are present in the organic phase: a discrete metal complex, a metal complex that has second-sphere (or outer-sphere) interactions (e.g., hydrogen bonding), ion pairs or clusters of ions, and reverse micelles (Figure 3).

Insert Figure 3 here

2.1.1. Complex formation

The formation of metal complexes that are soluble in the organic phase in a SX system is perhaps the most common, and best understood, mode of action, and can be described by coordination chemistry, namely the bonding between a metal cation and a ligand (sometimes known as first-, primary-, or inner-sphere bonding). The formation of discrete metal complexes can occur in a variety of ways, but primarily by acid-base chemistry (pH swing, Eq. 1) or neutral salt formation (solvation, Eq. 2).

$$M^{n+}_{(aq)} + n\,HL_{(org)} \leftrightharpoons [M(L)_n]_{(org)} + n\,H^+_{(aq)} \quad (1)$$

$$M^{n+}_{(aq)} + n\,X^-_{(aq)} + m\,L_{(org)} \leftrightharpoons [MX_n(L)_m]_{(org)} \quad (2)$$

One of the most studied systems that makes use of acid-base chemistry is the solvent extraction of copper using phenolic aldoximes and ketoximes (Figure 4). It is estimated that 20% of global copper supply is delivered using these types of reagents in solvent extraction processes [10]. This area has been extensively reviewed, so only recent advances in the chemical understanding of the mode of action are highlighted here [11].

Insert Figure 4 here

It was reported previously that the X-substituent of the phenolic oxime buttressed the hydrogen-bonding interaction between the phenolic oxygen atom and the adjacent oxime hydrogen atom, and that the nature of the X-substituent was a dominant effect on the strength of solvent extraction of Cu (Figure 4) [12, 13]. This is perhaps, surprising, as the bond dissociation energies of metal-ligand bonds are at least one order of magnitude greater than those of hydrogen bonds. Recently however, this was studied further by analysing similar Cu complexes by EPR (Cu^{2+} is d^9 with a single unpaired electron) and ^{1}H ENDOR (electron nuclear double resonance) spectroscopy, DFT calculations, and X-ray crystallography [14]. In this case, the ^{1}H ENDOR spectra are dominated by coupling of the unpaired electron to the azomethine and oximic protons, which provides information on the Cu…H distances for the various complexes and gives an indication of the strength of the hydrogen bond and Cu–N/O bonds. For X = aminomethyl, this represents a lengthening of the Cu–N/O bonds and hence a decrease in the bond strength. However, a strong buttressing effect is seen by X-ray crystallography, and the strength of extraction of Cu by this ligand is anomalous. As such, the deprotonation energies of the pro-ligands, the binding energies of the Cu complexes, and the formation energies of the Cu complexes were evaluated computationally. From these data, it is seen that the strength of Cu extraction is related to a combination of factors and not only hydrogen-bond buttressing. For example, for the X = Br ligand, the ease of deprotonation due to the added EWG and the strong buttressing effect of the *ortho*-Br compensate for the weaker binding energy of the ligand to Cu that arises from the reduced basicity of the NO^- donor

atoms. Overall, this provides a sound chemical reasoning on the strength of solvent extraction exhibited by the phenolic oximes reagents.

Phenolic pyrazoles (Figure 4, right) have also been evaluated as extractants for Cu and the structures of the resulting complexes studied by X-ray diffraction and DFT calculations [15]. As with the phenolic oximes above, the presence of groups with the ability to buttress the phenolic oxygen–oxime hydrogen bond were shown to be the strongest extractants, although the ease of deprotonation of the pro-ligand is again a significant factor. Also, the pyrazole N–H donor is less accessible to the *ortho*-substituent compared to the equivalent in the phenolic oximes, and only for *ortho*-nitro substitution is strong buttressing of the hydrogen bonding seen, with otherwise minimal bonding seen from natural bond order analysis.

Tripodal polyamines based on the tris(2-aminomethyl)amine (tren) platform have potential in solvent extraction, as the NN_3 donor set can be tuned by N-substituent variation. This is exemplified by a series of tren ligand with aromatic N-substituents which were used in the solvent extraction of transition metals at buffered pH 7.4 [16]. These ligands showed selectivity for Ag(I) and Zn(II) over Co(II), Ni(II), and Cd(II), which was attributed to a combination of lipohilicity of the ligand and the stability constants of the extracted complexes.

The separation, or partitioning, of lanthanides (Ln) from actinides (An) is a significant issue in nuclear-waste remediation, as the lanthanides are efficient neutron absorbers and so inhibit the fission of recycled nuclear fuels and hence the transmutation of the highly radioactive trans-actinides. As the 5f orbitals have greater radial extension compared to the 4f orbitals, it is thought that the actinide-ligand bond has a higher covalent contribution than the analogous lanthanide-ligand bond [17, 18]. This feature would provide a basis for Ln/An separation through the use of ligands that favor covalent interactions over ionic interactions. While the significance of aromatic nitrogen heterocycles in the separation of actinides from lanthanides is long understood, the chemical understanding of the extraction mechanisms is being increasingly studied [19].

Ligands such as triazinyl bipyridines and phenanthrolines (Figure 5) have an array of ‘soft’ nitrogen donor atoms and therefore should favour a more covalent bonding than ionic bonding to a metal.

Insert Figure 5

As such, these ligands have displayed significant An/Ln separation factors; for example, BTPhen exhibits D_{Am} >1000 compared with D_{Eu} <10 from nitric acid [20]. The locked conformation of BTPhen results in very fast extraction kinetics, high efficiency, and high selectivity compared to its Bipy analogue, with the fast kinetics due to the higher surface activity of the ligand at the phase interface [21]. The mode of extraction follows the metal salt route (Eq. 2) with the formation of the 2:1 ligand:metal complex $[Eu(NO_3)(BTphen)_2][NO_3]_2$, as verified by X-ray crystallography. Solution ^{1}H NMR (Nuclear Magnetic Resonnance) dipolar paramagnetic shift analysis of the Yb(III) perchlorate analogue showed the presence of a 2:1 ligand:metal complex. Good correlation between experimental and computed peak shifts is also seen in the presence of nitrate, but the solution structure could not be determined with accuracy. Clearly, the nitrate anions must be associated with the cationic complex to ensure solubility in the organic phase and MD calculations of the Yb(III) analogue showed that the structure is not coordinatively saturated.

The effect of electronic variation of BTPhen on the extraction of An/Ln was studied (Figure 4, right) and showed order-of-magnitude differences in distribution ratios while maintaining a high separation factor ($SF_{Am/Eu}$ *ca.* 110) [22]. The extraction mechanism was studied for Cm(III) by time-resolved laser-induced fluorescence spectroscopy (TRLFS). At low ligand concentrations (10^{-7} M), the 2:1 L:M complex was seen to form slowly (over 11 days), with the primary species in solution being solvated Cm(III) and the 1:1 complex $Cm(BTPhen)^{3+}$. However, at ligand concentrations more representative of an extraction process (10^{-2} M), only the 2:1 complex $Cm(BTPhen)_2^{3+}$ is observed. The effect of HNO_3 concentration on the extraction profile was studied, showing that the basicity of the ligand is an important factor. Distribution ratios were seen to decrease on increasing the basicity of the ligand (e.g., X = OMe, p*K*a = 3.9), the opposite was seen for less basic ligands (e.g. X = Cl, p*K*a = 1.7), indicating that it is the neutral ligand that transports the metal from the aqueous to the organic phase.

A raft of ligands containing combinations of pyridine and triazene groups with a variety of substituents have been reported and their modes of action studied [19]. The general extraction mechanism is by metal salt formation, and the use of lipophilic anions such as 2-bromohexanoic acid is seen to greatly enhance the extraction properties. More recently, the coordination properties of the zwitterionic nitrogen heterocyclic ligand HN_4bipy towards lanthanides and actinides was evaluated (Figure 6) [23].

Insert Figure 6 here

In this case, HN_4bipy contains an ionizable hydrogen atom, so the ligand coordinates to the Lewis acidic metal as the anion N_4bipy^-, resulting in a stronger, electrostatic interaction. The Sm(III) complex was studied by X-ray crystallography, showing the 2:1 L:M complex $Sm(OH)(OH_2)_2(N_4bipy)_2$ in the solid state. The formation of Cu(III) and Eu(III) complexes of HN_4bipy were analysed by TRLFS which showed 2:1 and 3:1 L:Cm complexes and 1:1 and 3:1 L:Eu complexes in solution. Determination of the stability constants of these complexes indicated a separation factor between Cu(III) and Eu(III) of *ca*. 500, an order of magnitude greater than the analogous alkylated ligands, RN_4bipy. As expected, the presence of 2-bromohexanoic acid only weakly competes with HN_4bipy, although more lipophilic versions of HN_4bipy would be required for its use in solvent extraction processes.

An alternative method for the separation of actinides from lanthanides is through the non-selective extraction of Ln and An into the organic phase (e.g., using the diglycolamide *N*,*N*,*N*',*N*'-TetraOctylDiGlycolAmide, TODGA) followed by selective back-transfer of the An into the aqueous phase through the use of hydrophilic ligands, for example, as shown in the TALSPEAK process [24], ALSEP process [25], and more recently the *i*-SANEX process [26, 27]. Recently, tetra-sulfonated versions of the above BTPhen ligands have been developed and exploited in this context (Figure 7, left) [28].

Insert Figure 7 here

The addition of TS-BTPhen to the 0.5 M nitric acid aqueous phase in the extraction of Eu(III) and Am(III) by TODGA resulted in a separation factor of 616, compared to that of 3.5 in the absence of TS-BTPhen, significantly higher than the polyaminocarboxylate ligands used in the TALSPEAK process. Interestingly, the selectivity of TS-BTPhen for Am over Eu is similar to that seen for the hydrophobic analogue BTPhen, which suggests that the coordination chemistry of this ligand class is preserved in both aqueous and organic phases.

As an alternative to TS-BTPhen, which suffers from radiolytic damage, the CHON-compliant, water-soluble (bis)triazine phenanthroline ligands have been developed and evaluated as selective Am(III) back-extractants (Figure 7, right) [29, 30]. Ligands such as BTrzPhen are able to differentiate between An and Ln, with separation factors of 36-47 favouring the An at low

ligand concentrations. The solid-state structure of the Eu complex showed a 2:1 L:M ratio, similar to those seen for other An/Ln complexes extracted into an organic or aqueous phase. As mentioned above, the diglycolamide TODGA (Figure 8) and its variants are used as neutral solvent extractants for Ln/An extraction and separation, often in combination with phosphorus acids.

Insert Figure 8 here

As such, the role of these compounds in the mechanism of extraction has been studied, and is driven fundamentally by the formation of the metal salt $LnX_3(L)_n$ (Eq. 2). While the solid-state structures determined by X-ray diffraction show a ligand:metal ratio of 3:1, with outer-sphere anions, the structures of these complexes in solution has only recently been determined. The Eu(III) complex $[Eu(TODGA)_3][BiCl_4]$ was analysed by EXAFS (Extended X-Ray Absorption Fine Structure), and it was found that the cation $[Eu(TODGA)_3]^{3+}$ is present in solution, with no anion coordinated to Eu due to the rigidity of the chelating O_9-donor set [31]. This analysis parallels the structures determined in the solid state and implies that the variation in extraction seen across the Ln series is likely defined by the differences in the hydrophobicity due to outer-sphere effects of different charge-balancing anions; this may well suggest that aggregation or reverse-micelle formation is operative in these systems (see later). The subtle energetic variation that underpins lanthanide extraction by diglycolamides were investigated by EXAFS and DFT calculations. As with the previous examples, EXAFS shows that the $[Ln(TODGA)_3]^{3+}$ structure is maintained in solution across the lanthanide series. On this basis, DFT calculations on a series of diglycolamides and related ligands showed that an interplay between steric strain and coordination energies gives rise to the nonlinear trend in lanthanide cation complexation; this shows the importance of strain energies to the design of the chelating ligands [32]. More recently, EXAFS and MD/DFT calculations on lanthanide diglycolamide extraction have shown that chloride or nitrate anions reside in clefts derived from the lipophilic arms of the diglycolamide ligands, through outer-sphere electrostatic and non-classical C-H hydrogen-bonding interactions [33]. Also, subsequent work has shown that the co-extraction of water modifies the location of the anions within the structure which subsequently effects the separation of the light *vs*. heavy rare-earth elements [34]. Similar

microhydration effects have been proposed recently for the mode of action of solvent extraction of lanthanides using ammonium ionic liquids [35].

The speciation of Eu and Nd complexes formed in an organic phase comprising the C-functionalised malonamide DMDOHEMA (see Figure 12) and the phosphoric acid D2EHPA was analysed using ESI-MS, TRLFS, NMR, EXAFS, and DFT calculations in order to gain insight into synergism in Ln recovery by solvent extraction [36]. It was found that the order of addition of the individual extractants was important to the speciation. The phosphoric acid D2EHPA undergoes acid-base chemistry with the Ln cation to produce $M(L)_3(HL_3)$ complexes in the organic phase and the subsequent addition of the malonamide causes the loss of neutral D2EHPA ligands (HL) forming a more lipophilic mixed-ligand complex. However, starting from malonamide-loaded organic phase, the Ln-containing species has attendant water and nitrate anions which are replaced on addition of D2EHPA. As with the examples above, it is clear that while metal complexes of a defined coordination sphere are formed, the outer-sphere interactions are more difficult to probe, and so whether the extraction occurs by a molecular or micellar mechanism remains ill-defined.

EXAFS was used to probe solution speciation in the extraction of Nd(III) from ethylene glycol (EG) into dodecane using the phosphine oxide Cyanex 923. In this case, the mechanism of extraction was shown to be through the formation of the salt $Nd(L)_3(NO_3)_3(EG)$, and the used of this extraction procedure allowed the separation of heavy and light rare earth elements [37].

While the fate of the anion in many of the above structures is unknown, namely in the inner- or outer-coordination sphere, or in a reverse micelle, ligands that incorporate both metal cation and anion binding sites are able to transport metal salts as well-defined molecules from the aqueous into the organic phase. This approach requires an appreciation of both coordination and supramolecular chemistry in the design of metal-ligand and anion-receptor sites.

A series of N-donor ligands, such as macrocyclic cyclen, with attendant urea anion-binding sites has been prepared (Figure 9) and are shown to selectively solvent extract copper as the salts $[Cu(L)(SO_4)]$ in preference to Co(II), Ni(II), and Zn(II), albeit without the loading capacity for an efficient SX process [38]. In the solid state, the cyclen coordinates the metal cation, and the urea hydrogen bonds to the anion. In the case of the copper complex, the sulfate interacts

with both the Cu centre and the urea, whereas for Zn the two nitrate anions are bound separately.

Insert Figure 8 here

2.1.2. Ion pairs and metalates

In many cases, the transfer of the metal species from the aqueous to the organic phase occurs as an ion pair or anion that does not form a coordination complex. That is, the interactions between the extractant and the metal species are electrostatic or supramolecular (hydrogen bonding, π-bonding); in this case, the extractant is best described as a receptor that ultimately forms a host-guest assembly on interaction with the metal species.

Calix[4]pyrroles can be viewed as ditopic receptors, as they can bind metal cations and anions simultaneously and have been used as extractants for cesium halides [39], but unlike those described above (Figure 8), no coordinate bond is formed between the metal cation and a donor atom, with only hydrogen bonding, electrostatic, and ionic Cs-arene π interactions present (Figure 10) [38].

Insert Figure 10 here

The simple octamethyl calix[4]pyrrole binds CsCl and CsBr in a 1:1:1 ligand:metal:halide stoichiometry on extraction into nitrobenzene from aqueous solution by an ion-pairing mechanism; in contrast, $CsNO_3$ behaves as a fully dissociated extraction system. Cation binding is absent without anion binding, as the strong interaction between the anion and receptor promotes organisation of the receptor into a cone conformation of appropriate cavity size for the Cs cation, as seen by X-ray crystallography. A similar calix[4]pyrrole receptor with *meso*-hexyl substituents has also been shown to act as a receptor for CsBr [40]. Combined solution EXAFS, DFT, and MD studies on this system indicate that the toluene solvent interacts strongly with the Cs^+ cation, capping the coordination sphere through a cation-π-interaction, providing evidence that supposed 'non-interacting' solvents may be more active in the structural chemistry than first envisaged (Figure 10, right).

The solvent extraction of anionic metalates from acidic media such as HCl using organic, protonatable bases is effective at achieving separation of base and precious metals (Eq. 3).

This is perhaps surprising as the chemical separation is achieved through the formation of supposedly weak supramolecular interactions such as hydrogen bonds, and therefore little control over the host-guest assemblies formed in the organic phase would be expected. However, recent work has shown that control of these outer-sphere interactions can have a profound effect on the thermodynamic stability of the host-guest assembly, so effecting separation in a solvent extraction system.

$$MX_y^{n-}{}_{(aq)} + n\,H^+{}_{(aq)} + n\,L_{(org)} \leftrightharpoons [(HL)_nMX_y]_{(org)} \qquad (3)$$

Pyridine-amides have been shown to be effective extractants for base metals such as Zn(II) and Co(II) [41, 42]. In these systems, the number of amido-substiuents proximate to the pyridine is important to the selectivity of metalate over halide. On protonation of the pyridine, the resulting receptor is stabilised by an internal bifurcated hydrogen bond which provides a diffuse array of N-H and C-H bonds for interaction with the metalate (Figure 11). This 'soft' set of hydrogen bonds interacts preferentially with the 'soft' chlorometalate in preference to the 'hard' chloride which is in excess in the aqueous phase.

Insert Figure 11 here

The solid-state structure shows the formation of at least four N–H and C–H hydrogen bonds per receptor and the metalate $ZnCl_4^{2-}$. DFT calculations support the solid-state structure and show that the formation constant for the Zn assembly is greater than that for the Co assembly. This feature, along with the formation constant for $ZnCl_4^{2-}$ being higher than that for the Co analogue $CoCl_4^{2-}$ results in favourable separation.

Other, more-simple receptor designs that make use of the hydrogen-bond chelate effect shown above have been reported (Figure 11, right) [43]. Intrinsic to this design is the feature that, on protonation, a stable, six-membered *pseudo* chelate is formed. These receptors were found to show high selectivity for $ZnCl_4^{2-}$ over $FeCl_4^-$, an *anti*-Hofmeister bias, and Cl^- which was rationalised using hybrid DFT calculations and is dependent on the number of N-H hydrogen bonds and the ease of protonation of the amido-amine through the formation of a proton-chelate structure.

Both amido-amine and amido-pyridine compounds have been found to act as receptors for perrhenic acid, facilitating the liquid-liquid extraction of perrhenate into the organic phase. In this case, higher order clusters are present in solution, with ESI-MS (Electrospray Ionization-

Mass spectrometry) showing ions representative of $(HL)_2(ReO_4)_2$ host-guest assemblies [44]. This is supported in the solid-state X-ray crystal structure in which two protonated pyridine diamide receptors are organised such that two perrhenate oxoanions are encapsulated by an array of polarised N–H and C–H hydrogen bonds. Also of note here is the propensity of the neutral amido-amine to decompose under strongly acidic conditions, which implies that these particular compounds act as synergistic extractants, namely a primary amide $RC(O)NH_2$ coupled with an ammonium salt $R'_2NH_2^+$.

Mono-, bi-, and tripodal receptors derived from tris(aminoethyl)amine (tren) or tris(aminopropyl)amine (trpn) have been compared in the extraction of the precious chlorometalate $PtCl_6^{2-}$ [45, 46]. These reagents were designed to recognised the outer-coordination sphere of $PtCl_6^{2-}$ through the triangular faces of the octahedron, although ultimately formed 2:1 receptor:chlorometalate assemblies in which the proton is encapsulated by receptor at the axial amino nitrogen. Higher extraction of $PtCl_6^{2-}$ is seen with urea-substituents compared to amide and sufonamides, and tripodal amide receptors are more effective than bi- or mono-amides. In some cases, the formation of a proton-chelate similar to those described above results in very high selectivity for $PtCl_6^{2-}$ over chloride, templating of the receptor and providing positively polarised N-H and C-H hydrogen bonding arrays.

Recently, attempts were made to exploit amido-amine and amido-pyridine (e.g. PDA, Figure 11) compounds in the extraction of lanthanides as their chlorometalates [47]. Previous reports on the extraction of lanthanides by ionic liquids such as quaternary ammonium salts under high aqueous salt concentrations have suggested the formation of lanthanide chloro- or nitratometalates LnX_6^{3-} in the organic phase. While successful uptake of $PtCl_6^{2-}$ by PDA from 6 M HCl was seen, no uptake of lanthanides or of other 3− chlorometalates such as $IrCl_6^{3-}$ occurred. DFT calculations showed that the substitution of aquo ligands by chloride, nitrate, and sulfate ligands in the aqueous phase is unfavourable, instead forming outer-sphere assemblies such as $[La(OH_2)_9][Cl]_x$ in which the aquo ligands are retained in the inner-sphere. This highlights the importance of the Hofmeister bias and the need to consider the stability of metal species in the aqueous phase, not only that of the metal species transported into the organic phase.

2.1.3. Reverse Micelles

The types of amphiphiles used in solvent extraction experiments can assemble into nanoscale structures allowing hydrophilic and hydrophobic environments to co-exist that can be understood as soft matter. These nanoscale structures are very different from the discrete, molecular entities described above, and so require different techniques and strategies to understand their formation.

The transfer of $Eu(NO_3)_3$ from an aqueous phase into a water-poor, amphiphile-in-oil system (c-functionalised malonamide DMDOHEMA in heptane) was studied due to its nonclassical distribution behaviour (Figure 12) [48]. Here, the mechanism of extraction was found to be a combination of coordination and supramolecular/colloid chemistry in which structural evolutions in the organic phase change the properties of the solvent. As such, initial extraction is through the formation of metal salts $Eu(L)_3(NO_3)_3$ in the organic phase, as shown by EXAFS and TRLFS measurements. Subsequently, vapour pressure osmometry (VPO) and small/wide angle X-ray scattering (SAXS/WAXS) studies, combined with MD simulations showed the formation of reverse micelles, which draw water and the amphiphile into nanoscale domains. Further increasing the Eu(III) concentration results in further aggregation of the reverse micelles thought to be due to Eu-NO_3 interactions.

Insert Figure 12

Tributyl phosphate (TBP) is an industrially relevant solvating extractant used to separate plutonium and uranium from nuclear fuel waste and is prone to form third phases under high acid and metal concentrations due to its amphiphilic nature and propensity to form reverse micelles [49]. While the study of these colloidal systems by X-ray and neutron scattering techniques is increasingly common [50], pulsed-field-gradient NMR spectroscopy has only recently been used to study the shape and size of metal-containing aggregates [51]. This diffusion NMR method is complementary to small-angle scattering techniques and was used to study the interactions between TBP aggregates containing uranium or zirconium cations and HNO_3 in a dodecane diluent. The aggregate sizes were found to be similar in size to those evaluated by diffraction methods, but in contrast a repulsive interaction between the aggregates was discovered, suggesting that this feature should be included in models to improve diffraction data simulations.

Structural insight into the multinuclear speciation of Ce(IV) in the TBP/dodecane solvent extraction system was recently reported [52]. A combination of XANES, EXAFS, and SAXS analysis indicated that tetranuclear Ce(IV)-oxo cores in reverse micelle structures of *ca*. 6 Å diameters are formed, solvated by TBP. At low cerium concentrations (<0.14 M), these reverse micelles are randomly and homogeneously dispersed with some short-range interactions, whereas at high Ce concentration (1.5 M) a third phase is formed comprising correlated, long-range, percolated micellar aggregates.

2.1.4. Conclusion

It is becoming increasingly clear that an appreciation of the fundamental chemistry that underpins solvent extraction is necessary to make significant advances is the design and development of new processes that can deal with more economically and environmentally efficient metal recovery from a diversity of primary and secondary sources. Understanding the modes of action of known ligands, receptors, and solvating agents will help in the design of new extractants, and requires knowledge of coordination chemistry, supramolecular chemistry, and colloidal science and a vast array of spectroscopic, diffraction, and computational techniques. While much of the previous work in this area has gleaned information using slope analysis and X-ray crystallography, there is now an increasing trend to evaluate solution structure by mass spectrometry, NMR spectroscopy, TRFLS, DFT and MD calculations, and solution diffraction techniques such as EXAFS, SAXS, and SANS. While more 'sporting', these techniques are better able to describe solution structure and so provide a better reflection of the mechanism of extraction.

2.2. The role of physicochemistry for a rational design of new extractants

The physicochemistry involved in liquid-liquid extraction processes is complex because of the presence of an interphase between the aqueous solution and the organic solution, the non-ideality of the aqueous and organic phases and the numerous chemical equilibria that can occur in each of these two phases (hydrolysis, precipitation, complexation, aggregation, etc.). In order to describe precisely the phenomena of metal transfer from the aqueous phase to the organic phase (or from the organic phase to the aqueous phase in the case of a desextraction), it is important to characterize finely the equilibria taking place in each of these phases and to determine the apparent thermodynamic constants associated with these equilibria. The comprehension of the physicochemistry of solvent extraction and a fine

knowledge of the speciation in aqueous and organic phases will bring useful information to design new extractants and to model metal extraction in order to build tools which can be used to optimize solvent extraction processes (Figure 13).

Insert Figure 13

Physicochemical models could be advantageously combined with engineering models in order to develop smart processes, namely processes that can adapt to the nature of composition of the feed solution so that the process always works under optimized conditions. The smart processing approach is particularly relevant for treating resources like spent materials or tailings for which the composition can change drastically over the time and the location.

By way of illustration, the development of physicochemical models for the recovery of uranium from concentrated phosphoric acid by a synergistic mixture of bis-(2-éthylhexyl)phosphoric acid (D2EHPA) and tri-*n*-octylphosphine (TOPO) is presented below. Such a physicochemical model could be particularly interesting in order to anticipate changes of the formulation of the extraction solvent (for instance because of the difference of solubility of D2EHPA and TOPO in the aqueous phase which leads to potential deformulation).

If new insights on the understanding of uranium extraction and U/Fe selectivity with D2EHPA/TOPO were brought recently [53-57], the mechanisms of uranium-selective extraction with these synergistic systems remain poorly understood. Empirical research has thus been mostly performed to propose better synergistic mixtures by changing the cation exchanger and/or the neutral-donor ligand in the reference D2EHPA/TOPO solvent.

Extraction occurring at approximately 5 M H_3PO_4 for Wet Phosphoric Acid (WPA), cation exchangers with very low pK_a are privileged to compete with H_3PO_4 acidity. Carboxylic acids are for instance not suitable for uranium extraction from this media. Many different cation exchangers, belonging to phosphoric, phosphonic, or even phosphinic acids, have thus been tested in combination with TOPO for uranium(VI) extraction from WPA. Among them, dibutyl dithiophosphoric acid (HDBDTPA), bis(2-ethylhexyl)dithiophosphoric acid (D2EHDTPA) [58], dioctyl (DOPPA) [59] and dinonyl phenyl phosphoric acid (DNPPA) [60], bis(2-ethylhexyl) phosphinic acid (B2EHPA) [61], and (2-ethylhexyl)phosphonic acid mono-2-ethylhexyl ester (PC88A) [62] were used in mixture with TOPO (Figure 14).

Insert Figure 14 here

The extraction efficiency of uranium increases logically with the acidity of the cation exchanger in the following order: phosphinic acid<phosphonic acid<phosphoric acid<thiophosphoric acid. Derivatives with an ether function on the hydrophobic part of the extractant (D2EHOEPA and BiDiBOPP) were also synthesized and showed that the presence of additional oxygen atoms increases uranium distribution ratio compared to D2EHPA [63].

On the other hand, several neutral-donor ligands such as tri-*n*-butylphosphate (TBP), di-*n*-butyl butyl phosphonate (DBBP) [60, 64, 65] or di-*n*-hexyl-methoxyoctylphosphine oxide (di-*n*-HMOPO) [56] were tested in combination with D2EHPA to substitute TOPO in the reference mixture. As with cation exchangers, uranium extraction increases with the basicity of the neutral ligand (phosphate < phosphonate < phosphine oxide) and with the introduction of an ether group on the phosphine oxide ligand (Figure 15).

Insert Figure 15 here

Other synergistic mixtures containing a cation exchanger such as dibutyldithiophosphoric acid (DBDTPA), bis(2-ethylhexyl) dithiophosphoric acid (D2EHDTPA), bis(1,3-dibutoxyprop-2-yl)phosphoric acid (BiDiBOPP), dinonylphenyl phosphoric acid (DNPPA), or (2-ethylhexyl) phosphonic acid mono-2-ethylhexyl ester (PC88A) and a neutral synergistic molecule such as di-*n*-hexyl-methoxyoctylphosphine oxide (di-*n*-HMOPO), dibutyl butyl phosphonate (DBBP), tri-*n*-butyl phosphate (TBP), or octyl(phenyl)-*N*,*N*-diisobutylcarbamoyl methyl phosphine oxide (CMPO) were also tested for uranium extraction from WPA [63].

The development of physicochemical model is very useful to understand the physicochemistry of extraction, the extraction equilibria and to evaluate the speciation inorganic phase. For instance, Chagnes et al. developed a physicochemical model to describe uranium(VI) extraction by D2EHPA/TOPO, BiDiBOP/di-*n*-HMOPO, or other derivatives from 5.3 M phosphoric acid [64]. In this model, the dimerization of the acidic cationic extractant HL and the association between HL and the solvating agent S were taken into account by considering the formation of $(HL)_2$, $(HL)_2S$, $(HL)_2S_2$, and a supramolecular complex $(HL)_5S$:

$$2\overline{HL} \leftrightharpoons \overline{(HL)_2} \quad (3)$$

$$\overline{(HL)_2} + \bar{S} \leftrightharpoons \overline{(HL)_2S} \quad (4)$$

$$\overline{(HL)_2} + 2\bar{S} \leftrightharpoons \overline{(HL)_2S_2} \quad (5)$$

$$\overline{HL} + 2\overline{(HL)_2} + \bar{S} \leftrightharpoons \overline{(HL)_5S} \quad (6)$$

Furthermore, it was considered that uranium(VI) is extracted according to the following equilibria:

$$UO_2^{2+} + 2\overline{(HL)_2} \leftrightharpoons \overline{UO_2(HL_2)_2} + 2H^+ \quad (7)$$

$$UO_2^{2+} + 2\overline{(HL)_2} + \bar{S} \leftrightharpoons \overline{UO_2(HL_2)_2S} + 2H^+ \quad (8)$$

$$UO_2^{2+} + \overline{(HL)_2} + \bar{S} \leftrightharpoons \overline{UO_2(HL)_2S} + 2H^+ \quad (9)$$

By implementing these equilibria in the physicochemical model and by considering no significant changes in uranium complexation by phosphates and hydrogenophosphates since phosphoric acid concentration and pH are constant, the distribution ratios of uranium(VI) between 5.3 mol L^{-1} phosphoric acid and HL/S diluted in Isane IP 185 (a grade of aliphatic kerosene) were calculated as a function of the organic-phase composition (Figure 16). A good agreement was obtained between the calculated distribution ratios of uranium(VI) and the experimental ones.

Insert Figure 16 here

This model has been applied to the BiDiBOPP-di-*n*-HMOPO system. It appears that a good agreement between calculated and experimental data is obtained by considering the same set of extraction equilibria as for the D2EHPA/TOPO system (Figure 16).

Such a model can be used to predict and optimize liquid-liquid extraction a function of extraction solvent composition for many mixtures of organophosphorus cation exchangers and solvating agents. However, it can work only at constant phosphoric acid concentration. By combining this physicochemical model with an equation of state to describe the variation of activity coefficents in phosphoric acid, it is possible to perform predictive calculations as a function of extraction solvent

composition and phosphoric acid concentration. Such a model was also developed by Chagnes et al. [67, 68] (Figure 17).

Insert Figure 17

The existence of the predominant species $UO_2(HL)_2L_2S$ predicted by the physicochemical model was demonstrated by means of time-resolved laser-induced fluorescence spectroscopy (TRLFS). It is particularly interesting to highlight that the TOPO molecule in this species is located in the first solvation shell of uranium(VI), as it was also confirmed by DFT calculations (Figure 18).

Insert Figure 19

The presence of such species in which cation exchanger and solvating agent are both in the first solvation shell of uranium(VI) paves the way to the development of bifunctional ligands as those recently developed by CEA (see paragraph 2.3.1 below as a case study).

2.3. Case studies

2.3.1. Design of new extractants for uranium recovery from wet phosphoric acid

Since significant amounts of uranium (50–200 ppm) are contained in phosphate rocks, its recovery from industrial WPA is an important goal in order to decontaminate phosphoric acid and, at the same time, valorize uranium for the nuclear industry. According to the world's reserves, 4 Mt of uranium would be available from natural phosphate rocks [69], which constitutes an important secondary source for uranium production. Separation of uranium from concentrated phosphoric acid is however challenging and requires intensive R&D. Several hydrometallurgical processes based on solvent extraction have been developed since 1970, and some of them operated at an industrial scale. The first successful process for uranium recovery from WPA was developed by Oak Ridge National Laboratory and is based on the selective extraction of U(VI) by a synergistic combination of a cation exchanger (D2EHPA) and a neutral-donor ligand (TOPO) in an organic phase [70]. This process, later modified by Cogema (URPHOS process) [71, 72] allowed to produce hundreds of tons of uranium from WPA in the 1980s and 1990s. Uranium was sufficiently purified but required two extraction cycles to reach the specifications for nuclear-grade uranium.

Two other processes were also developed at an industrial scale and used phosphorus extractants to extract U(IV). The OPAP process [73] is based on a mixture of mono and dioctylphenyl phosphoric acid, while the OPPA process uses dioctylpyrophosphoric acid for uranium(IV) extraction [74, 75]. All these processes showed efficient extraction of U(IV) or U(VI) depending on the synergistic mixture, but different drawbacks such as insufficient uranium/impurities (iron in particular) selectivity, additional steps for uranium redox control, or degradation of the extractant under hydrolysis (for OPPA) were pointed out and limited their performances. These processes should thus be improved to be more competitive in order to be economically attractive for uranium production according to the current uranium price.

Improvement of these processes involves the design of new extracting molecules to bring higher affinity, selectivity, and robustness than the classical formulations used in the former industrial processes. Extensive research and development has been performed in this field to study new extractant molecules for the selective extraction of uranium from WPA [63, 76].

Several criteria must be taken into account to define efficient molecules capable to extract uranium from concentrated phosphoric acid solutions. First, as phosphate anions are scarcely extracted in organic phase, extraction by solvation (metal salt extraction) using a neutral ligand (i.e., uranium extraction by TBP from HNO_3) is not possible in that case. Moreover, very few anionic complexes being formed between phosphate anions and uranium, anion exchange is also not suitable. Cationic exchange is thus the main extraction mode enabling uranium extraction from phosphoric acid. However, phosphate anions being strong complexing agents for uranium, a cation exchanger is generally not powerful enough by itself to compete with phosphate complexation in aqueous phase. Another binding function is therefore required to help uranium transfer to the organic phase by un-complexing uranyl cation from phosphate ions and water molecules and completing uranium coordination sphere. This effect is commonly explained by an additional solvation that would increase the uranium complex lipophilicity and its extractability in organic phase.

Two different approaches can be therefore considered to tackle this issue: either using a combination of two molecules, a cation exchanger in addition to a new neutral-donor ligand, so-called a synergistic mixture (as already implemented in the Oak Ridge process) or designing new multifunctional ligands combining both cation exchanger and neutral-donor functions on the same molecular architecture.

As mentioned previously in this chapter, a large number of synergistic systems has been developed and tested for uranium extraction from phosphoric acid media. If improvements of uranium extraction efficiency compared to the Oak Ridge Process were observed with some of these new synergistic combinations, these formulations remain insufficient to reach the desired selectivity for minimizing the impurities concentrations in the yellow cake (iron in particular) in only one extraction cycle. Besides, the process must operate at the optimum synergistic ratio of the mixture to reach the best performances while extraction efficiency and selectivity properties of synergistic mixture are generally very sensitive to a slight deviation of this ratio. These reasons reinforced the need to develop new selective extractants instead of synergistic mixtures to fit industrial objectives.

This part of the chapter introduces the design of multifunctional ligands that combine both the cation exchanger (phosphoric, phosphonic acid) and the neutral donor functions (phosphine oxide, amide, …) on the same molecular structure. The use of a single molecule combining the properties of the two functions of the synergistic mixture is interesting not only to simplify the process but also to potentially enhance uranium distribution ratio and U/impurities selectivity. The idea is to pre-organize the two functions for uranium coordination in order to increase the complex stability by favouring the entropic contribution (well known “chelate effect”).

Based on this approach, the first bifunctional extractant reported in the literature for uranium extraction from phosphoric acid was synthesized by Warshawsky et al [77]. O-methyldihexylphosphine oxide O’-hexyl-2-ethyl phosphoric acid (MDHPOH2EPA), depicted in Figure 20, includes a phosphoric acid as a cation exchanger while phosphine oxide acts as a neutral donor. A higher uranium extraction than in the Oak Ridge system was obtained with this extractant but U/Fe selectivity remains insufficient. Moreover, third-phase formation was observed in extraction conditions with this system.

Insert Figure 20 here

Pursuing this way, new bifunctional ligands, carrying a phosphonic acid group as cation exchanger and an amide group as neutral-donor function, were designed by Turgis et al. [78]. Amidophosphonic acids, also named carbamoyl-alkylphosphonic acids, were first synthesized and tested towards uranium extraction from WPA. The influence of different modifications of

the ligand structure (nature of the alkyl chains attached to the amide group, spacer length between the two functions, steric hindrance on the spacer, etc.) was studied through a structure/efficiency approach and correlated to extraction efficiency and U/Fe selectivity. In solvent extraction, these structural modifications strongly influence the efficiency and selectivity of the extractant but also some important physicochemical parameters such as the ligand partitioning into the aqueous phase, the ligand solubility in aliphatic diluents, the metal complexes solubilities in the organic phase (limit towards third-phase formation, cruds formation at the interface upon extraction or stripping, etc.), the organic-phase density and viscosity (impacting the phase settling and separation) or the ligand stability under hydrolysis. The best balance between the total number of carbons and the nature of hydrogenocarbon groups (linear or branched alkyl chains, short or long chains, aliphatic or aromatic groups, etc.) should be found to design the best ligand fulfilling the main criteria defined for the process development.

It appears that uranium extraction was maximized with 2-ethylhexyl chains on the amide function and a methylene bridge between the amide group and the phosphonic acid while U/Fe selectivity was enhanced by steric hindrance after alkylation of the methylene by a phenyl group. DEHCPBA (*N*,*N*-di-2-ethylhexyl-carbamoylbenzylphosphonic acid) exhibits higher distribution ratios than the D2EHPA-TOPO solvent, but U/Fe separation factor remain still too low (<200), requiring additional efforts to define the best molecular design.

Based on the promising results obtained on DEHCPBA and carbamoylmethylphosphonic acids, amido phosphonate ligands were studied after monosaponification of the corresponding amido phosphonic acids. Keeping 2-ethylhexyl chains on the amide group and a methylene bridge between the two extracting functions, several amido phosphonate ligands were synthesized by changing the nature of the alkylchain grafted on the spacer and on the phosphonate group. It appears that the presence of monosaponified phosphonate moiety in combination with the addition of an octyl pendant chain on the methylene bridge dramatically enhance the uranium extraction efficiency and the U(VI)/Fe(III) selectivity [79, 80].

The so-called DEHCNPB (butyl-1-[*N*,*N*-bis(2-ethylhexyl)carbamoylnonyl]phosphonic acid) reported in Figure 21 was put forward in regards to the outstanding results obtained for the selective extraction of uranium compared to the D2EHPA/TOPO synergistic solvent.

Insert Figure 21 here

Indeed, uranium distribution ratio and U(VI)/Fe(III) selectivity are more than 30 times and between 15 and 50 times higher than the reference D2EHPA/TOPO respectively. Furthermore, DEHCNPB extracts uranium selectively from the other impurities (Mo, V, Al, …) present in genuine industrial phosphoric acid with unequaled performance. This molecule was thus selected for process development [81, 82].

Since, other "autosynergistic" bifunctional ligands have been recently developed for uranium extraction by substituting the amide donor group of amido phosphonates by a phosphine oxide [83]. Keeping similar alkyl chains than those optimized in the case of DEHCNPB, new phosphine oxide-phosphonate ligands were synthesized and compared with DEHCNPB and the reference D2EHPA/TOPO mixture. Uranium was highly and selectively extracted by DEHNPB phosphine oxide phosphonate from a genuine industrial phosphoric acid solution with a better U/Fe separation factor compared to D2EHPA/TOPO. The U/Fe selectivity remains nevertheless lower in comparison to the amido-derivative.

2.3.2. Chemical design in gold recovery by urban mining

The case for the recycling of waste electronic and electrical equipment (WEEE) is compelling. In 2012, 49 million tons of WEEE were generated globally, primarily by the developed countries, containing at least 57 elements many of which are present in concentrations significantly higher than in their primary ore deposits and are listed as critical resources [84]. This is compounded by the exponential growth of the mobile electronics market coupled with the reduced lifetime of devices. While it is clear that prevention and reuse are preferable options in the e-waste management hierarchy and 3R policy (Figure 22), the recycling of WEEE would not only solve issues with landfill disposal and the leaching of hazardous elements, but also has enormous potential as a resource for valuable and critical materials through 'urban mining' [85], potentially closing-the-loop and creating a circular economy. This has resulted in a series of global initiatives such as the Restriction of Hazardous Substances Directive (RoHS), the EU WEEE Directive 2012/19/EU, and Solving the E-waste Problem (StEP) [86, 87].

Insert Figure 22 here

The recycling of WEEE using physical and chemical methods has been reviewed and is found to be complex, requiring dismantling, crushing, and classification of the materials followed by separation and refining steps by, for example, pyro-, hydro-, and/or biohydrometallurgical routes [84, 88]. While significant progress has been made in separating metallic from nonmetallic fractions and in finding economical uses for these latter waste products (e.g., fillers and composites), the recovery of individual metals remains an issue due to the difficulty in adapting technologies used to recover metals from primary ore feed streams for use in a WEEE feed stream. Such an issue is particularly true in pyrometallurgy since many metals are lost in the slags and it explains why more and more industries try implementing hydrometallurgy rather than pyrometallurgy. The eventual increase of the cost due to the implementation of hydrometallurgy instead of pyrometallurgy may be paid by the recovery of many metals by hydrometallurgy in most cases.

The environmental impacts of WEEE treatment are also important to understand and have been evaluated by life-cycle analysis [89]. In this case, a hydrometallurgical process that was analysed comprised two different leaching steps, in nitric acid and aqua regia, followed by electrodeposition for the recovery of Cu, Ag, and Au and adsorption steps for Ni and Sn recovery. The analysis found that the nitric acid leaching process has the highest environmental impact, contributing highly to eutrophication, acidification, human toxicity, global warming (from its synthesis), and abiotic depletion, with the adsorption steps proving inefficient and so also a high contributor. Furthermore, LCA evaluation on the recycling of smartphones show it to have a net benefit in terms of carbon dioxide equivalents [90]. It is important to note here that improvements in the chemistry of leaching, separation, and refining steps that occur in a hydrometallurgical process would benefit the overall environmental (and economic) impact of WEEE recycling.

This part of the chapter will focus on recently reported research for the recovery of gold from WEEE, in particular research that has used chemical understanding to inform on the mechanism of operation [91]. Even though gold is only present in small quantities in WEEE, for example ca. 0.25 g per smartphone, it represents the most value to recover [92]. WEEE is an important gold resource; it is estimated that 1 ton of smartphones contains 300 g of gold, which is a significantly more concentrated resource than the primary ore, of which one ton would yield 3–7 g [93]. Furthermore, it is also estimated that the recovery of gold from WEEE

would decrease the environmental and mining footprint along with savings of 17,000 tonne per tonne in carbon dioxide emissions.

2.3.2.1. Leaching.

As stated above, leaching of precious metals such as gold from WEEE is environmentally impactful as it necessitates the use of strong acids under oxidising conditions, for example HNO_3 or aqua regia (1:3 HNO_3:HCl), or the use of extremely toxic chemicals such as cyanide/O_2 to dissolve gold by forming the Au(I) complex $Au(CN)_2^-$ [94]. Alternatively, leaching chemicals such as thiourea/Fe^{3+}, thiosulfate/O_2, and KI/I_2 are used, but their costs and environmental hazards are seen as prohibitive. Bio-oxidation and cyanidation are also possible methods for gold leaching [94]. The use of dithiobiuret reagents have proved beneficial for simultaneous leaching and extraction of gold from aqua regia and direct leaching into partially water-immiscible solvents such as CH_3CN in the presence of HCl/H_2O_2. Oxidative leaching using H_2O_2/H_2SO_4 is suitable for the leaching of Cu from waste printed circuit boards (WPCBs), providing both good Cu recovery and separation from the WPCB resin, but its potential for leaching other metals has not been explored [95]. Simple acid leaching in air has also been studied and dilute HCl (1.0 M) shown to lixiviate gold and other metals to a high degree from WPBCs provided suitable levels of the oxidant (O_2) is present and agitation occurs [96].

Very recently, a new, low-toxicity method for the leaching of gold from WPCBs using a synergistic mixture of N-bromosuccinamide (NBS) as an oxidant and pyridine (py) as a ligand has been described (Figure 23) [97] Experimental variation of the reagents and conditions showed that gold dissolution was maximised (90%) using 10 mM NBS, 100 mM py, at pH 8.2 and 25 ^oC, and contrasts to only 77% gold dissolution using KI/I_2; the cost of these latter reagents is 20x greater.

Insert Figure 23 here

The mechanism of gold dissolution was investigated and showed that the first step was oxidation of the gold surface by NBS at the relatively low potential of −0.854 V to form the Au(III) complex $AuBr_4^-$. This metalate then reacts with pyridine to form the neutral complex $AuBr_3$(py) due to a high binding constant of 10^5–10^6 M. It is therefore clear that both NBS and py are required to maximise gold leaching (i.e., synergism occurs) and that the use of low concentrations of NBS and py are important to the efficacy of the system.

This procedure has proved effective in separating gold from other metals present in WEEE, with 90% gold recovery compared with 40% of other metals such as Ni, Sb, Zn, Mg, Cu, Sn, Al, and Fe. When leaching gold from the surface of Ni-coated Cu CPU pins, the selectivity increases due to the formation of a Ni_xBr_y passivating surface, which inhibits further Ni and Cu oxidation.

The dilute nature of the NBS and py reagents was found to mitigate against mammalian toxicity, showing 100% viability in mammalian models compared to 0% when dosed with more traditional reagents. Similar attenuation of toxicity was seen in aquatic creature models, making the NBS/py an attractive, environmentally benign alternative to conventional gold leaching methods.

2.3.2.2. Precipitation of Au(III) and Au(0).

Leaching metals from WEEE yields a pregnant leach solution (PLS) that generally contains a mixture of metals that require separation, unless some separation process has operated at the leaching stage. Selectivity in separation is a key challenge to a hydrometallurgical metal recovery process, and a knowledge of coordination chemistry, supramolecular chemistry, and redox chemistry is important in designing a suitable system. One separation method is through precipitation and has been employed extensively in gold recovery, either carrying out separation as Au(III) or Au(I) complexes or by precipitation as Au(0) using carbonaceous- or bio-sorbents [92]. Gold deposition is also important in other fields where, for example, the size of the Au(0) nanoparticles formed in TiO_2/Au materials is key to their efficacy as catalysts in a variety of chemical reactions [98].

Recently, the use of polyaniline reductants (conducting polymers) was studied for the recovery of gold from a PLS of WEEE [99], based on earlier chemistry that showed that the rate of Au(0) deposition was dependent on the surface area on the polyaniline and its intrinsic oxidation state [100]. In the former example, polyanilines were immobilised on supporting materials such as cotton fibers and proved effective at Au(0) deposition due to the electroless cycling of leucoemeraldine, emeraldine, and pernigranile during Au(III) reduction in aqueous HCl. Alternatively, glow discharge lamps have been used to reduce metals with positive standard reduction potentials, favouring separation of Au from Cu, Zn, and Fe [101]. In this case, the separation of Au(0) was facilitated through the use of poly(vinylpyrrolidone) which, under the aqueous conditions used, forms a film on the surface of the solvent in which Au(0) is embedded. Also, the use of reduced graphene oxide (GO) hydrogels to precipitate Au(0)

from Au(III) solutions has been reported [102]. Here, GO was reduced by wild-type *Shenwanella oneidensis* MR-1 resulting in a biologically assembled GO hydrogel which could reduce Au(III) to Au(0) nanoparticles that become embedded in the hydrogel, with Au and Pd recovered preferentially from Cu, Zn and Ni.

Perhaps one of the most exciting chemical advances in this area is the use of supramolecular chemistry to favour the self-assembly of gold precipitates for the selective isolation of gold from other metals. In one example, the addition of α-cyclodextrin (α-CD) to $KAuBr_4$ in water resulted in the spontaneous precipitation of a one-dimensional supramolecular complex with an extended chain superstructure $\{[K(OH_2)_6][AuBr_4]\subset(\alpha\text{-CD})_2\}_n$ (Figure 24) [103].

Insert Figure 24 here

Single-crystal X-ray diffraction studies showed that a perfect match in molecular recognition between $[AuBr_4]^-$ and α-CD occurs, with axial orientation of the anion within the cyclodextrin cavity favouring a highly specific second-sphere electrostatic and hydrogen-bonding interaction between the $[AuBr_4]^-$ anion and the $[K(OH_2)_6]^+$ cation. In the structure, the $[K(OH_2)_6]^+$ cation is encapsulated by the secondary faces of two α-CDs whereas in other adducts the cations are coordinated by OH groups and glucopyranosyl O atoms in the CDs. This feature explains the differences of precipitation yield when using β- or γ-cyclodextrins instead of α-cyclodextrin and when using different gold salts such as Na, Cs, or $RbAuCl_4$. Indeed, out of 24 combinations of salt:cyclodextrin, only three result in precipitation: α-cyclodextrin with either K, Cs, or $RbAuCl_4$.

Metal-organic frameworks (MOFs) are porous materials that can be constructed using increasingly well-defined synthetic methods that make use of metal centres as tectons for bridging ligands. While their physical and chemical properties have been exploited in, for example, gas absorption and catalysis, respectively, their ability to sequester metals selectively is more rare. Recently, however, MOFs that incorporate sulfur-donor atoms within the porous cavities have been prepared and exploited in gold recovery [104]. In this case, the MOF is constructed rationally using dinuclear copper(II) complexes of a chiral bis(L-methionine)oxalamide ligand as a tecton in which the *anti*-configuration adopted by the ligand (Figure 25a) favours chain growth and, on the addition of Ca(II) cations, causes curvature

(Figure 25b) and the formation of the MOF. The MOF contains hexagonal channels of *ca*. 0.3 nm diameter that are decorated by L-methionine arms, which act as ligands for both Au(I) and Au(III). As such, soaking the MOF in water solutions containing $AuCl_3$ or AuCl results in gold uptake, forming the thioether complexes (RS)AuCl and (RS)$AuCl_3$ within the porous network. In the case of Au(I), the X-ray crystal structure shows the expected linear geometry for the (RS)AuCl complexes, along with short Au…Au distances of 3.04 Å indicative of aurophilic interactions (Figure 25c).

Insert Figure 25 here

These materials are highly selective for gold over other metals in solution. Soaking the MOF in an equimolar mixture of $AuCl_3$, $NiCl_2$, $CuCl_2$, $ZnCl_2$, $AlCl_3$, and $[Pd(NH_3)_4]Cl_2$ showed rapid uptake of Au(III), maximised after 30 minutes, with no uptake of other metals observed. The recovered gold can be released from the MOF by soaked the Au-loaded material in a sulfur-containing solvent such as dimethylsulfide, thus recycling the MOF for further gold uptake.

2.3.2.3. Solvent extraction of Au(III).

Solvent extraction (SX) is an attractive process for recovering metals from WEEE for, as long as the metals are leached, the PLS can be treated with a variety of reagents to separate and recover *all* of the metals sequentially. In principle, this would lead to complete recycling of the metals in WEEE with zero metal waste and, with recycling of the reagents used in SX processes, would provide excellent mass balance. If a single metal is targeted, SX offers significant environmental advantages over energy- and capital-intensive pyrometallurgical methods [3].

The solvent of extraction of gold from primary ores can be carried out from halide leach solutions using commercial reagents such as methyl isobutyl ketone (MIBK), dibutyl carbitol (DBC), or 2-ethylhexanol (2-EH) [105]. While the recovery of gold is efficient using these reagents, selectivity, safety, and mass balance issues are seen, and the chemistry that underpins their mode of action is poorly understood. As such, the development of new compounds that can selectively transport gold from aqueous to organic phases in a SX experiment remain desirable.

Several tertiary amides have been investigated as reagents for the solvent extraction of gold from HCl solutions (Figure 26).

Insert Figure 26 here

The two tertiary amides DOAA and DOLA which contain different chain-length substituents were evaluated for gold transfer into 4:1 dodecane/ethyl hexanol from aqueous HCl in the presence of other metals including Pd(II), Pt(IV), Rh(III), Fe(II), Cu(II), Ni(II), and Zn(II) [106]. Good selectivity for Au was seen at lower HCl concentrations (<3.0 M), and the strength of extraction was higher for DOAA than DOLA. However, DOAA formed a third phase under these conditions, which was absent when using DOLA. Extractions using this latter reagent also allowed back-extraction using water (70%), whereas DOAA required the use of thiourea, thus affecting the overall mass balance. While these reagents show promise in gold extraction, the mode of action of extraction was not evaluated.

In a more recent study, a larger series of tertiary amides was evaluated for gold recovery from HCl solutions [107]. As with the above systems, extractions were carried out from mixtures of metals, Au(III), Pt(IV), Pd(II), Rh(III), Cu(II), and Ni(II), into 4:1 dodecane/2-ethylhexanol, and similar performance was seen with rapid phase transfer, quantitative (for MBHA, DHOA, and DHEHA), and dependent on the length and symmetry of the hydrocarbon substituents, with unsymmetrical substituents (MBHA) better than symmetrical substituents (DHOA, DHEHA). In this case, the analysis of the slopes of linear log *D* vs. log[L] plots ([L] = concentration of extractant) indicated that two reagent molecules were required for every Au transferred, suggesting a basic stoichiometry of $HAuCl_4(amide)_2$ as the extracted species.

While the use of tertiary and secondary amides in metal recovery by solvent extraction is well advanced, primary amides have been little studied in this area [108], perhaps due to the premise that the presence of multiple N–H groups would encourage extensive hydrogen bonding and so limit solubility in the organic phase. However, the use of amidoamines in base metal solvent extraction and from this the recognition that controlling hydrogen-bonding interactions can aid selectivity in the transfer of a metalate from the aqueous to organic phase [91] resulted in a new study on the use of primary amides in the solvent extraction of gold [109]. It was found that transfer of Au(III) from aqueous HCl into a 0.1 M primary amide MDMHA solution in toluene (Figure 26) was rapid and quantitative, and unusually, with straightforward back-extraction occurring using water. This reagent is also highly selective, extracting Au(III) from a mixture of Fe(III), Cu(II), Zn(II), Sn(II), and Ni(II) at concentrations

similar to those found in a typical smartphone (Figure 27). Compared to MIBK, DBC, and 2-EH, MDMHA shows increased selectivity, and unlike the commercial reagents can be used in a diluent.

Insert Figure 27 here

Importantly, the chemistry that underpins the mode of extraction was studied in detail by a variety of analytical and spectroscopic techniques. Analysis of the slopes of linear log *D* vs. log[L] plots suggested that at a minimum a 1:2 Au:L stoichiometry was operating, namely the formation of $HAuCl_4(MDMHA)_2$ similar to that described above (Figure 28).

Insert Figure 28 here

However, decreasing the gold concentration in the aqueous phase led to non-integer slopes (2.5), which implies that the speciation in the organic phase is variable. Karl-Fischer analysis of the organic phase showed that water is not transferred with gold, as no increase in the water concentration is seen on increased gold loading.

Analysis of the Au-loaded organic phase by EXAFS spectroscopy showed that $AuCl_4^-$ is present, and that there were no close contacts between individual $AuCl_4^-$ complexes (Figure 28). This may imply that simple $HAuCl_4(MDMHA)_2$ ion pairs are present, but analysis of the organic phase by ESI-MS showed a preference for cluster formation. In the mass spectrum (Figure 28), the dominant gold species have a generic formula of $[H(MDMHA)_2(AuCl_4)_n(H\text{-}MDMHA)_{n-1}]$ (where n = 1–4); that is, a basic 1:2 $HAuCl_4(MDMHA)_2$ complex exists, but higher-order clusters are favoured and represented by the further addition of $HAuCl_4$(MDMHA) units.

Further insight into the chemical speciation was provided by DFT and MD calculations (Figure 28). From these, it was found that aggregation into Au:amide clusters occurs readily in a solvated toluene box, with 4:10 $HAuCl_4$/MDMHA calculations showing a variety of structural motifs in which hydrogen-bonded amides are able to bridge discrete $AuCl_4^-$ centres through electrostatic and hydrogen-bonding to defined edges of the square-planar gold cation. As such, the combined analytical and spectroscopic analysis provides clear evidence for the spontaneous formation of supramolecular clusters facilitated by the simple primary amide, MDMHA.

2.3.2.4. Conclusion

The recovery of gold from WEEE is an important starting point for the complete recycling of these complex materials due to its economic value and relatively straightforward separation from other metals. However, one of the key technological advances that remains to be solved is its efficient, nontoxic, and potentially selective leaching from WEEE components but, as described above, some progress is being made in this area. The combination of efficient leaching with selective precipitation or solvent extraction techniques would result in a powerful process that could not only recover gold, but also other valuable or toxic metals from WEEE, so moving towards the closed-loop WEEE economy desired by society. As described above, chemists have made significant headway into understanding the mode of action of hydrometallurgical processes by studying the structures of the chemical compounds in aqueous, organic, or precipitated phases. The structural detail identified from these coordination and/or supramolecular chemical studies may point towards new designs of extractants that make use of recurring motifs to provide enhanced and efficient separation. Even so, while significant advances have been made in hydrometallurgical separation, their integration into a whole process needs to be considered, which relies upon continued input from, and collaboration between, chemists, biologists, engineers, economists, and the industries involved.

3. Flowsheet optimization

The efficiency of solvent extraction plants depends on various factors such as flow rates, concentration, nature of the feed solution, flowsheets, *etc*. Especially powerful is the ability to implement scrubbing stages to effect higher product purity. The modification of any one of these factors strongly affects the performance of an extraction plant. Nevertheless, sometimes, it may be necessary to modify one of these factors to face up to many problems such as low solvent loading, poor quality product, formation of cruds, precipitates, and emulsions, radiolysis or chemical stresses, etc. [110]. Classical counter-current flowsheets, for example, 4 mixers-settlers in the extraction section and 3 mixers-settlers in the stripping section, constitute a typical set-up implemented in solvent extraction plants for the recovery of metals from ores. Nevertheless, they are not always the best set-up when configured in this way, and it is possible to increase the metal production, product purity, and concentration factor.

3.1. Effect of flowrates on flowsheet performances

For instance, the extraction efficiency of the two flowsheets reported in Figure 29 are drastically different. Modelling can bring useful information to select the best flowsheet and optimize it to take advantage of the increasingly powerful emergent chemistry.

Insert Figure 29 here

The flowsheet 4_3 is a classical countercurrent flowsheet whereas the other flowsheet, quoted 22_11*, is an unconventional flowsheet with two extraction-stripping loops. Each loop corresponds to two mixers-settlers in the extraction stage and one mixer-settler in the stripping stage. Chagnes et al. investigated the influence of the flowsheet for uranium extraction [111].

The influence of the solvent flow rate (S), the feed solution flow rate (F) and the stripping solution flow rate (F') on the residual fraction (defined as the uranium concentration in the raffinate (x_4) over its concentration in the inlet feed solution, $f = x_4/x_0$) for the classical flowsheet (4_3) and the unconventional flowsheet (22_11*) is displayed in Figure 30.

Insert Figure 30 here

The residual fraction decreases when the solvent flow rate increases and remains constant after a threshold value of S equal to 29 $m^3.h^{-1}$ for both flowsheets. The classical counter current flowsheet permits to reach a residual fraction close to zero for solvent flow rates higher than 29 $m^3.h^{-1}$, whereas f remains close to 0.5% at the same range of solvent flow rates. A sharp decrease of residual fraction is also observed when the stripping solution flow rate increases but the drop in f is more important with the 4_3 configuration: f is close to zero with the 4_3 flowsheet and f = 1.1% with the 22_11* flowsheet at F '= 5.5 $m^3.h^{-1}$.

The classical counter-current flowsheet ensures to reach a feed solution flow rate of 115 $m^3.h^{-1}$ without a significant increase of the residual fraction. No threshold value of f is observed with the 22_11* flowsheet when the feed solution flow rate is lower than 130 $m^3.h^{-1}$. The sharp increase of f, at solvent flow rates higher than 115 $m^3.h^{-1}$, can be explained by the saturation of the solvent extraction which cannot extract more uranium, as there are not enough mixers-settlers to treat the feed solution in the stripping stage at high S/F' ratio. On

the other hand, no saturation phenomenon is observed with the 22_11* flowsheet even if the residual fraction with 22_11* remains higher than with 4_3 before the threshold value (F = 115 $m^3.h^{-1}$). The 22_11* flowsheet does not enhance the extraction efficiency, but it permits to avoid the saturation of the organic phase above 130 $m^3.h^{-1}$.

3.2. Influence of degradation on flowsheet performance

Solvent extraction processes may undergo stresses such as radiolysis or chemical degradation. For example, chemical degradation of trioctylamine and tridecanol in *n*-dodecane as a diluent may occur due to the presence of strong oxidant metal ions in the feed solution such as vanadium(V) [112]. In the case of vanadium(V), the degradation occurs as follows: (i) Vanadium(V) is extracted by Alamine® 336 from aqueous phase to organic phase; (ii) the strong oxidation power of V(V) is responsible of the oxidation of the modifier (tridecanol) to carboxylic acid according to a radical mechanism; (iii) the preceding radicals react quickly with Alamine 336 to form dioctylamine (DOA) as a degradation product [112]. Furthermore, the degradation of Alamine 336 to dioctylamine is responsible for a drop of extraction efficiency, as dioctylamine is a less efficient extractant for uranium(VI) than is trioctylamine.

By including the physicochemistry of degradation into the flowsheet simulation, it is possible to investigate the sturdiness of candidate flowsheets against chemical degradation of the solvent. Figure 31 displays the sturdiness of the 4_3 and 22_11* flowsheets against the degradation progress, that is, DOA molar fraction in the Alamine 336-tridecanol-*n*-dodecane system [113].

Insert Figure 31 here

There is no influence of the chemical degradation on the extraction efficiency for the classical counter-current flowsheet as long as the molar fraction of DOA is lower than 0.1. At higher DOA molar fractions, the residual fraction increases linearly. The use of DOA instead of Alamine 336 is responsible of an extraction loss equal to 8.8%.

Therefore, the implementation of the 22_11* flowsheet in a solvent extraction process for the recovery of uranium(VI) from sulphuric acid media permits to enhance the resistance of the solvent extraction process toward chemical degradation. In fact, a slow increase of residual fraction is observed when the molar fraction of DOA in organic phase increases (Figure 3). The use of a second loop in the extraction process permits to increase strongly the resistance of

the process against degradation. Works are in progress for testing other configurations to understand the origin of the enhancement of the flowsheet sturdiness. It may be supposed that the effect of the solvent extraction degradation may be counterbalanced by the increase of the extraction capacity of unconventional flowsheets.

3.3. Combining chemistry and engineering for flowsheet optimization

Likewise, modelling tools for optimizing flowsheets and operation conditions have been used by CEA in order to optimize a flowsheet for extracting uranium(VI) from wet phosphoric acid by using the new bifunctional molecules DEHCNPB (see above). A chemical model was elaborated for uranium and iron extraction by DEHCNPB in order to precisely simulate the behavior of these elements in the SX process whatever the concentrations of uranium, phosphoric acid or DEHCNPB concentration are. Based on experimental extraction isotherms and, when it was possible, on speciation studies of uranium and iron both in phosphoric acid solutions and in the organic phase, extraction equilibria were proposed, and extraction constants were adjusted to fit the experimental values. First, uranium and iron speciation in 5 M H_3PO_4 were calculated by selecting the main equilibria formed in aqueous solution among the different equilibria reported in the literature [114, 115]. Miguirditchian et al. [116] considered four equilibria to describe uranium speciation in phosphoric media while two equilibria were sufficient for iron (Table 1).

Insert Table 1 here

Then, based on the speciation results obtained in organic phase, cation exchange for uranium(VI) by DEHCNPB was considered in its proton-dimer form. Extraction of uranium by 2.5 dimers of DEHCNPB (i.e., two dimers and one monomer) along with the formation of a bimolecular uranium complex (2:4) allowed reaching the best fit of the experimental isotherm. The global form of these equilibria and the associated thermodynamic constants are given by Eqs. 1–3.

It is usually rigorous to take into account activity coefficients in the aqueous phase to correct deviations from ideality in process conditions. Different theories such as the “simple solution” concept [117, 118] or SIT (Specific Interaction Theory) [119, 120] are, for instance, often used in nitric acid or sulfuric media to calculate activity coefficients. However, phosphoric acid being poorly dissociated, activity coefficients in the aqueous phase were supposed to be

constants in that case. Activity coefficients in the organic phase were also considered constants in the operating uranium concentration range to simplify the modelling.

$$UO_2^{2+} + 2.5(\overline{HY})_2 \leftrightharpoons \overline{UO_2Y_2(HY)_3} + 2H^+ \qquad K_{U1} = \frac{\left[\overline{UO_2Y_2(HY)_3}\right]\cdot\left[H^+\right]^2}{\left[UO_2^{2+}\right]\cdot\left[(\overline{HY})_2\right]^{2.5}} \quad (10)$$

$$2\,UO_2^{2+} + 2\,(\overline{HY})_2 \leftrightharpoons \left(\overline{(UO_2)_2Y_4}\right) + 4\,H^+ \qquad K_{U2} = \frac{\left[\overline{((UO_2)_2\,Y_4)}\right]\cdot\left[H^+\right]^4}{\left[UO_2^{2+}\right]^2\cdot\left[(\overline{HY})_2\right]^2} \quad (11)$$

Iron(III) extraction by DEHCNPB was also modelled by a cation-exchange mechanism involving a combination of a dimer and a monomer according to the following equilibrium:

$$Fe^{3+} + 1.5(\overline{HY})_2 \leftrightharpoons \overline{FeY_3} + 3H^+ \qquad K_{Fe} = \frac{\left[\overline{FeY_3}\right]\cdot\left[H^+\right]^3}{\left[Fe^{3+}\right]\cdot\left[(\overline{HY})_2\right]^{1.5}} \quad (12)$$

Extraction constants were optimized by minimizing the differences between experimental and calculated organic concentrations after application of the mass action law on each equilibrium. Mass balances were resolved in both phases in order to determine the free concentrations. The comparison between experimental and calculated data for the isotherm of uranium(VI) extraction is depicted on Figure 32. A very good agreement between experimental and calculated data is reached with an average deviation lower than 5%.

Insert Figure 32 here

The chemical model was than implemented into the PAREX simulation code [121] to calculate a flowsheet in order to perform a countercurrent laboratory run (Figure 33).

Insert Figure 33 here

Taking into account the objectives for uranium recovery and purification, an optimized flowsheet including three stages for uranium extraction, three stages for iron scrubbing, one stage for water scrubbing and four stages for uranium stripping was proposed. This flowsheet was tested in laboratory scale mixer-settlers from a genuine industrial phosphoric acid solution. More than 95% of uranium was recovered and very well decontaminated from iron and other impurities, confirming the high selectivity of DEHCNPB for uranium from WPA and the high potential of this new molecule for future industrial development.

Therefore, simulation tools based on the physicochemistry of solvent extraction is very useful to model and optimize processes. A deep understanding of the equilibria taking place in solvent extraction is the key to imagine new efficient processes.

3.4. Perspective in the development of tools for flowsheet optimization

In order to reduce OPEX, the process must be able to adapt to raw material composition and to anticipate issues. This is especially true for recycling processes as waste composition can dramatically vary throughout time and depending on the origin of the wastes. Indeed, waste composition changes depending on technology progress, country's economic health, location, etc. The implementation of engineering and chemical codes is the key to develop smart processes capable to adapt the operating conditions and the flowsheet automatically so that the process always operates under optimized conditions. The tools presented in the previous part can be viewed as preliminary blocks for an implementation in smart processes. However, the development of such models requires the acquisition of thermodynamic data, which can be time-consuming. Nevertheless, the time spent for developing the models and the associated database will be undoubtedly compensated by OPEX gain resulting from their use in hydrometallurgical processes.

The impacts of this approach on process performance can be drastically improved by combining physicochemical and engineering models with artificial intelligence (machine learning, deep-learning, big data) and Predictive Maintenance Technologies promoted by Advanced Manufacturing approach [122].

4. Conclusion

Extraction and valorization of metals are presently more difficult than in the past because of the complexity of new resources to process. These resources include poor and polymetallic ores (laterite-saprolite, pyrochlore, pegmatite, etc.), tailings, e-wastes (lithium-ion batteries, WEEE, etc.) ... It is therefore mandatory to develop new approaches and new strategies to reduce process cost and environmental footprint while keeping high performances. For this goal, many efforts must be paid to develop a holistic approach that includes geochemical cycle of the metals, concentration methods, extraction processes, environmental impact studies and market analysis. In particular, the technical and economic feasibility of the process rely on flowsheet design. The latter depends on resources composition and technologies involved in the extraction-separation stages. In the case of solvent extraction processes, performances

depend both on engineering and chemistry. It is therefore of great importance to optimize these engineering and chemistry at the same time. Regarding the chemistry, the extractants are at the center of solvent extraction processes. Extractant design needs to have a fine description of the speciation in the leach solution and metal-ligand interaction and coordination. Obviously, the extractant molecule is not alone in the solvent and its environment must be taken into account as well (diluent effect, molecular and supramolecular association). The physicochemistry is complex and modelling tools are especially adapted to investigate the influence of the chemical structure of a molecule on these properties. Regarding flowsheet design, the combination of physicochemical and engineering models is the key to develop disruptive and optimized flowsheets. Thanks to these integrated approach, the flowsheet can adapt to changes in compositions or external constraints, and therefore, operate under optimal conditions. The next generations of hydrometallurgical processes should also rely on artificial intelligence and Predictive Maintenance Technologies promoted by Advanced Manufacturing approach since these technologies will likely lead to smart processing which will be able to adapt to changes in operation conditions and to fix immediately the main issues. This approach will likely drastically reduce operating costs, maintenance costs, energy consumption and environment impact by keeping the process optimized at any time.

5. References

1. Scholl, D.S. and Lively R.P. 2016 , *Nature*, 2016, 532, 435-437.
2. Tasker, P.A. ; Plieger, P. G. and West, L. C. 2005. Comprehensive Coordination Chemistry II, eds. J. A. McCleverty and T. J. Meyer, Elsevier Ltd, Oxford, ch. 9.17, pp. 759-808.
3. Izatt, R. M.; Izatt, S. R.; Bruening, R. L. ; Izatt, N. E. and Moyer, B. A. 2014. Chemical Society Reviews, 43, 2451-2475
4. Xie, F. Zhang; T. A.; Dreisinger D. and Doyle, F. 2014. Minerals Engineer*ing*, 56, 10-28.
5. Chagnes, A. 2015. Fundamentals in electrochemistry and hydrometallurgy, eds A. Chagnes, J. Swiatowska In *Lithium Process Chemistry: Resources, Extractions, Batteries and Recycling*, 41-80. Amsterdam: Elsevier.
6. Chagnes, A.; Moncomble, A. and Cote, G. 2013. Solvent Extraction and Ion Exchange 31 (5), 499-518.
7. Prestianni, A.; Joubert, L.; Chagnes, A.; Cote, G.; Ohnet, M.N.; Rabbe, C.; Charbonnel, M.C. and Adamo, C. 2010. Journal of Physical Chemistry A. 114 10878-10884.

8. Prestianni, A.; Joubert, L.; Chagnes, A.; Cote, G. and Adamo, C. 2011. Physical Chemistry Chemical Physics 13, 19371-19377.
9. Turkington, J.R.; Bailey, P. J.; Love, J. B.; Wilson, A. M. and Tasker, P. A. 2013. Chemical Communications 49, 1891-1899
10. US Geological Survey, M. D. Doggett, Global Mineral Exploration and Production – The Impact of Technology, https://pubs.usgs.gov/circ/2007/1294/reports/paper10.pdf (accessed 5 July, 2018).
11. Wilson, A. M.; Bailey, P. J.; Tasker, P. A.; Turkington, J. R.; Grant, R. A. and Love, J. B. 2014. *Chemical Society Reviews* 43, 123-134.
12. Forgan, R. S.; Wood, P. A.; Campbell, J.; Henderson, D. K.; McAllister, F. E.; Parsons, S.; Pidcock, E.; Swart, R. M. and Tasker, P. A. 2007. Chemical Communications, DOI: 10.1039/B712278K, 4940-4942.
13. Forgan, R. S.; Roach, B. D.; Wood, P. A.; White, F. J.; Campbell, J. ; Henderson, D. K.; Kamenetzky, E.; McAllister, F. E.; Parsons, S.; Pidcock, E. ; Richardson, P.; Swart, R. M. and Tasker, P. A. 2011. Inorganic Chemistry 50, 4515-4522.
14. Healy, M. R. ; Carter, E. Fallis, I. A.; Forgan, R. S.; Gordon, R. J.; Kamenetzky, E.; Love, J. B.; Morrison, C. A.; Murphy, D. M. and Tasker, P. A. 2015. Inorganic Chemistry 54, 8465-8473.
15. Healy, M. R.; Roebuck, J. W. Doidge, E. D.; Emeleus, L. C.; Bailey, P. J.; Campbell, J.; Fischmann, A. J.; Love, J. B; Morrison, .C. A; Sassi, T.; White, D. J. and Tasker, P. A. 2016. Dalton Transactions 45, 3055-3062.
16. Wenzel, M.; Hennersdorf, F.; Langer, M.; Gloe, K.; Antonioli, B.; Buschmann, H.-J.; Lindoy, L. F.; Bernhard, G.; Gloe K. and Weigand, J. J.. 2017. Separation Science and Technology, DOI: 10.1080/01496395.2017.1302953, 1-9.
17. Kaltsoyannis, N. 2013. Inorganic Chemistry 52, 3407-3413.
18. Choppin, G. R., Journal of Alloys and Compounds 2002, 344, 55–59.
19. Panak P.J. and Geist, A. 2013. Chemical Reviews 113, 1199-1236.
20. Drew, M. G. B. ; Foreman, M. R. S. J.; Hill, C.; Hudson, M. J. and Madic, C. 2005. Inorganic Chemistry Communications 8, 239-241.
21. Lewis, F. W.; Harwood, L. M.; Hudson, M. J.; Drew, M. G. B.; Desreux, J. F. ; Vidick, G.; Bouslimani, N.; Modolo, G.; Wilden, A.; Sypula, M.; Vu, T.-H. and Simonin, J.-P.. 2011. Journal of the American Chemical Society 133, 13093-13102.
22. Edwards, A.C.; Wagner, C.; Geist, A.; Burton, N. A.; Sharrad, C. A.; Adams, R. W.; Pritchard, R. G.; Panak, P. J.; Whitehead, R. C. and Harwood, L. M. 2016. Dalton Transactions 45, 18102-18112.

23. Kratsch, J.; Beele, B. B.; Koke, C.; Denecke, M. A.; Geist, A.; Panak, P. J. and Roesky, P. W. 2014. Inorganic Chemistry 53, 8949-8958.
24. Weaver, B. and Kappelmann, F. A. 1964. TALSPEAK, A new method of separating americium and curium from the lanthanides by extraction from an aqueous solution of an aminopolyacetic acid complex with a monoacetic organophosphate or phosphonate. ORNL-3559.
25. Gelis, A. V.; Lumetta, G. J.; Ind. Eng. Chem. Res. 2014, 53, 1624−1631.
26. Paiva, A. P. and Malik, P. 2004. Journal of Radioanalytical and Nuclear Chemistry 261, 485-496.
27. Geist, A.; Müllich, U.; Magnusson, D.; Kaden, P.; Modolo, G.; Wilden, A. and Zevaco, T. 2012. Solvent Extraction and Ion Exchange 30, 433-444.
28. Lewis, F. W.; Harwood, L. M.; Hudson, M. J.; Geist, A.; Kozhevnikov, V. N.; Distle, P. and John, J. J. 2015. Chemical Science 6, 4812-4821.
29. Edwards, A. C.; Mocilac, P.; Geist, A.; Harwood, L. M.; Sharrad, C. A.; Burton, N. A.; Whitehead, R. C. and Denecke, M. A. 2017. Chemical Communications 53, 5001-5004.
30. Malmbeck, R. ; Magnusson, D . ; Geist, A. ;. Journal of Radioanalytical and Nuclear Chemistry, 2017 314, 2531–2538.
31. Antonio, M. R.; McAlister, D. R. and Horwitz, E. P. 2015. Dalton Transactions 44, 515-521.
32. Ellis, R. J.; Brigham, D. M.; Delmau, L.; Ivanov, A. S.; Williams, N. J.; Vo, M. N.; Reinhart, B.; Moyer, B. A. and Bryantsev, V. S. 2017. Inorganic Chemistry 56, 1152-1160.
33. Brigham, D. M. ; Ivanov, A. S. ; Moyer, B. A. ; Delmau, L. H. ; Bryantsev, V. S. ; Ellis, R. J. Journal of the American Chemical Society, 2017, 139, 17350−17358.
34. Baldwin, A. G. ; Ivanov, A. S. ; Williams, N. J. ; Ellis, R. J. ; Moyer, B. A. ; Bryantsev, V. S. ; Shafer, J. C., ACS Central Science, 2018, 4, 739−747.
35. Hunter, J. P. ; Dolezalova, S. ; Ngwenya, B. T. ; Morrison, C. A. ; Love, J. B. ; Metals, 2018, 8, 465.
36. Muller, J. M.; Berthon, C.; Couston, L.; Guillaumont, D.; Ellis, R. J.; Zorz, N.; Simonin J.-P. and Berthon, L. 2017. Hydrometallurgy 169, 542-551.
37. Batchu, N. K.; Vander Hoogerstraete, T.; Banerjee, D. and Binnemans, K. 2017. Separation and Purification Technology, 174, 544-553.
38. Carreira-Barral, I.; Mato-Iglesias, M.; De Blas, A.; Platas-Iglesias, C.; Tasker, P. A. and Esteban-Gomez, D. 2017. Dalton Transactions 46, 3192-3206.
39. Wintergerst, M. P.; Levitskaia, T. G.; Moyer, B. A.; Sessler, J. L. and Delmau, L. H. 2008. Journal of the American Chemical Society 130, 4129-4139.

40. Ellis, R. J.; Reinhart, B.; Williams, N. J.; Moyer, B. A. and Bryantsev, V. S. 2017. Chemical Communications 53, 5610-5613.
41. Ellis, R. J.; Chartres, J.; Henderson, D. K.; Cabot, R.; Richardson, P. R.; White, F. J.; Schröder, M.; Turkington, J. R.; Tasker, P. A. and Sole, K. C. 2012. Chemistry – A European Journal 18, 7715-7728.
42. Ellis, R. J.; Chartres, J.; Sole, K. C.; Simmance, T. G.; Tong, C. C.; White, F. J.; Schroder, M. and Tasker, P. A. 2009. Chemical Communications, DOI: 10.1039/B815895A, 583-585.
43. Turkington, J. R. ; Cocalia, V.; Kendall, K.; Morrison, C. A.; Richardson, P.; Sassi, T.; Tasker, P. A.; Bailey, P. J. and Sole, K. C. 2012. Inorganic Chemistry 51, 12805-12819.
44. Cokoja, M. ; Markovits, I. I. E., Anthofer, M. H.; Poplata, S. ; Pothig, A.; Morris, D. S.; Tasker, P. A.; Herrmann, W. A.; Kuhn F. E. and Love, J. B.. 2015. Chemical Communications, **51**, 3399-3402.
45. Warr, R. J.; Bell, K. J.; Gadzhieva, A.; Cabot, R.; Ellis, R. J.; Chartres, J.; Henderson, D. K.; Lykourina, E.; Wilson, A. M.; Love, J. B.; Tasker, P. A. and Schröder, M. 2016. Inorganic Chemistry 55, 6247-6260.
46. Bell, K. J.; Westra, A. N.; Warr, R. J.; Chartres, J.; Ellis, R.; Tong, C. C.; Blake, A. J.; Tasker, P. A. and Schröder, M. 2008. Angewandte Chemie International Edition 47, 1745-1748.
47. Doidge, E. D.; Carson, I.; Love, J. B.; Morrison, C. A. and Tasker, P. A. 2016. Solvent Extraction and Ion Exchange 34, 579-593.
48. Ellis, R. J.; Meridiano, Y.; Muller, J.; Berthon, L.; Guilbaud, P. ; Zorz, N.; Antonio, M. R.; Demars, T. and Zemb, T. 2014. Chemistry – A European Journal 20, 12796-12807.
49. Osseo-Asare, K. 1991. *A*dvances in Colloid and Interface Science 37, 123-173.
50. Ferru, G.; Gomes Rodrigues, D.; Berthon, L.; Diat, O.; Bauduin P. and Guilbaud, P. 2014. Angewandte Chemie International Edition 53, 5346-5350.
51. Baldwin, A. G., Yang, Y. ; Bridges, N. J. and Braley, J. C. 2016. The Journal of Physical Chemistry B, 120, 12184-12192.
52. Antonio, M. R.; Ellis, R. J.; Estes, S. L. and Bera, M. K. 2017. Physical Chemistry Chemical Physics 19, 21304-21316.
53. Beltrami, D.; Chagnes, A.; Haddad, M.; Laureano, H.; Mokhtari, H.; Courtaud, B.; Juge, S.; Cote, G. 2014. Hydrometallurgy 144-145, 207-214.
54. Beltrami, D.; Cote, G.; Mokhtari, H.; Courtaud, B.; Chagnes, A. 2012. Hydrometallurgy 129-130, 118-125.
55. Beltrami, D.; Mercier-Bion, F.; Cote, G.; Mokhtari, H.; Courtaud, B.; Simoni, E.; Chagnes, A. 2014. Journal of Molecular Liquids 190, 42-40.

56. Dourdain, S.; Hofmeister, I.; Pecheur, O.; Dufreche, J. F.; Turgis, R.; Leydier, A.; Jestin, J.; Testard, F.; Pellet-Rostaing, S.; Zemb, T. 2012. Langmuir 28 (31), 11319-11328.

57. Pecheur, O.; Dourdain, S.; Guillaumont, D.; Rey, J.; Guilbaud, P.; Berthon, L.; Charbonnel, M. G.; Pellet-Rostaing, S.; Testard, F. 2016. Journal of Physical Chemistry B 120 (10), 2814- 2823.

58. Fitoussi, R.; Musikas, C. 1980. Separation Science and Technology 15, 845-886.

59. Krea, M.; Khalaf, H. 2000. Hydrometallurgy 58, 215-225.

60. Singh, H.; Vijayalakshmi, R.; Mishra, S. L.; Gupta, C. K. 2001. Hydrometallurgy 59, 69-76.

61. Beltrami, D.; Chagnes, A.; Haddad, M.; Laureano, H.; Mokhtari, H.; Courtaud, B.; Juge, S.; Cote, G. 2013. Separaion Science and Technology 48, 480-486.

62. Singh, S. K.; Tripathi, S. C.; Singh, D. K. 2010. Separaion Science and Technology 45, 824.

63. Beltrami, D.; Cote, G.; Mokhtari, H.; Courtaud, B.; Moyer, B. A.; Chagnes, A. 2014. Chemical Reviews 114, 12002-12023.

64. Bunus, F. T. 1977. Talanta, 24, 117-120.

65. Chen, H. M.; Chen, H. J.; Tsai, Y. M.; Lee, T. W.; Ting, G. 1987. Industrial & Engineering Chemistry Research 26, 621-626.

66. Ginesty, C. 1983. Improved dialkylphosphoric acid-phosphine oxide synergistic systems for uranium recovery from phosphoric liquors, ISEC'83, Denver, USA.

67. Dartiguelongue, A., Provost, E., Chagnes, A., Cote, G., Fürst, W. 2016. Solvent Extraction and Ion Exchange 34 (3), 241-259.

68. Dartiguelongue, A., Provost, E., Chagnes, A., Cote, G., Fürst, W. 2016. Hydrometallurgy 165, 57–63.

69. Gabriel, S.; Baschwitz, A.; Mathonniere, G.; Elouet, T.; Fizaine, F. 2013. Annals of Nuclear Energy 58, 213-220.

70. Hurst, F.; Brown, K. B.; Crouse, D. J. 1972. Industrial & Engineering Chemistry Process Design and Development 11, 122-128.

71. Cogema, FR Patent 7720552, 1977.

72. Michel, P.; Ranger, G.; Corompt, P.; Bon, P. New process for the recovery of uranium from phosphoric acid., Proceedings of the International Solvent Extraction Conference ISEC 80, Liege, Belgium, 1980; p 80.

73. Hurst, F. J.; Crouse, D. J., 1974. Industrial & Engineering Chemistry Process Design and Development, 13, 286-291.

74. Khorfan, S., 1993. Chemical Engineering and Processing 32, 273-276.

75. Mc-Cready, W. L.; Wethington, J. A.; Hurst, F. J. 1981. Nuclear Technology 53, 344-353.

76. Singh, D. K.; Mondal, S.; Chakravartty, J. K. 1966. Solvent Extraction and Ion Exchange 34, 201-225.

77. Warshawsky, A.; Kahana, N.; Aradyellin, R. 1989. Hydrometallurgy 23, 91-104.

78. Turgis, R.; Leydier, A.; Arrachart, G.; Burdet, F.; Dourdain, S.; Bernier, G.; Miguirditchian, M.; Pellet-Rostaing, S. 2014. Solvant Extraction and Ion Exchange 32, 478-491.

79. Arrachart, G.; Aychet, N.; Bernier, G.; Burdet, F.; Leydier, A.; Miguirditchian, M.; Pellet-Rostaing, S.; Plancque, G.; Turgis, R.; Zekri, E. Patent WO 2013/167516 A1, 2013.

80. Turgis, R.; Leydier, A.; Arrachart, G.; Burdet, F.; Dourdain, S.; Bernier, G.; Miguirditchian, M.; Pellet-Rostaing, S. 2014. Solvent Extraction and Ion Exchange 32, 685-702.

81. Bernier, G.; Miguiditchian, M.; Pacary, V.; Bertrand, M.; Cames, B.; Hérès, X.; Mokhtari, H. New Process for the Selective Extraction of Uranium from Phosphoric Ores, ISEC, Wurzburg, Germany, 2014.

82. Miguirditchian, M.; Bernier, G.; Pacary, V.; Balaguer, C.; Sorel, C.; Berlemont, R.; Fries, B.; Bertrand, M.; Cames, B.; Leydier, A.; Turgis, R.; Arrachart, G.; Pellet-Rostaing, S.; Mokhtari, H.. 2016. Solvent Extraction and Ion Exchange 34, 274-289.

83. Leydier, A.; Arrachart, G.; Turgis, R.; Bernier, G.; Marie, C.; Miguirditchian, M.; Pellet-Rostaing, S. Recovery of uranium (VI) from concentrated phosphoric acid by “autosynergistic” molecules Hydrometallurgy 2017, *accepted*.

84. Kaya, M. 2016. Waste Management 57, 64-90.

85. Cui, J. and Zhang, L. 2008. Journal of Hazardous Materials 158, 228-256.

86. Jadhao, P.; Chauhan, G.; Pant, K. K. and Nigam, K. D. P. 2016. Waste Management 57, 102-112.

87. Chagnes, A.; Cote, G.; Ekberg, C.; Nilson, M. and Retegan, T. “Recycling of Waste Electrical and Electronic Equipment: Research, Development and Policies”, Elsevier, 2016, 212 pages.

88. (a) Chatterjee, A. and Abraham, J. 2017. International Journal of Environmental Science and Technology 14, 211-222; (b) Sun, Z.; Cao, H.; Xiao, Y.; Sietsma, J. ; Jin, W. ; Agterhuis, H.

and Yang, Y. 2017. ACS Sustainable Chemistry & Engineering 5, 21-40; (c) Priya, A. and Hait, S. 2017. Environmental Science and Pollution Research 24, 6989-7008; (d) Diaz, L. A.; Lister, T. E.; Parkman, J. A. and Clark, G. G. 2016. Journal of Cleaner Production 125, 236-244; (e) Dodson, J. R.; Parker, H. L.; Munoz Garcia, A. ; Hicken, A. ; Asemave, K.; Farmer, T. J.; He, H.; Clark, J. H. and Hunt, A. J.. 2015. Green Chem. 17, 1951-1965.

89. Iannicelli-Zubiani, E. M.; Giani, M. I. ; Recanati, F. ; Dotelli, G.; Puricelli, S. and Cristiani, C. 2017. Journal of Cleaner Production 140, 1204-1216.

90. Baxter, J.; Lyng, K.-A.; Askham, C. and Hanssen, O. J. 2016.Waste Management 57, 17-26.

91. (a) Wilson, A. M.; Bailey, P. J.; Tasker, P. A.; Turkington, J. R.; Grant, R. A. and Love, J. B. 2014. Chemical Society Reviews 43, 123-134; (b) Turkington, J. R .; Bailey, P. J.; Love, J. B.; Wilson, A. M. and Tasker, P. A. 2013. Chemical Communications. 49, 1891-1899.

92. Syed, S. 2012. Hydrometallurgy 115–116, 30-51.

93. Hagelüken, C. and Corti, C. W. 2010. Gold Bulletin 43, 209-220.

94. Karthikeyan, O. P. ; Rajasekar, A. and Balasubramanian, R. 2015. Critical Reviews in Environmental Science and Technology 45, 1611-1643.

95. Ou, Z. J. and Li, J. 2016. Waste Management 57, 57-63.

96. Jadhav, U. and Hocheng, H. 2015. Scientific Reports 5, 14574.

97. Yue, C. ; Sun, H. ; Liu, W.-J.; Guan, B. ; Deng, X.; Zhang, X. and Yang, P. 2017. Angewandte Chemie International Edition, 2017, 56, 9331-9335.

98. Zanella, R. ; Giorgio, S.; Henry, C. R. and Louis, C. 2002. The Journal of Physical Chemistry B 106, 7634-7642.

99. Wu, Y.; Fang, Q.; Yi, X.; Liu, G. and Li, R.-W. 2017. DOI: http://dx.doi.org/10.1016/j.pnsc.2017.06.009.

100. Ting, Y. P.; Neoh, K. G.; Kang, E. T. and Tan, K. L. 1994. Journal of Chemical Technology & Biotechnology 59, 31-36.

101. Li, M.; Sun, Q. and Liu, C.-j. 2016. ACS Sustainable Chemistry & Engineering 4, 3255-3260.

102. He, Y.-R.; Cheng, Y.-Y.; Wang, v and Yu, H.-Q.. 2015. Chemical Engineering Journal 270, 476-484.

103. (a) Liu, Z. , Frasconi, M.; Lei, J. ;. Brown, Z. J ; Zhu, Z. ; Cao, D.; Iehl, J.; Liu, G; Fahrenbach, A. C.; Botros, Y. Y. Farha, O. K.; Hupp, J. T.; Mirkin, C. A. and Fraser Stoddart, J. 2013. Nature

Communications 4, 1855; (b) Liu, Z.; Samanta, A.; Lei, J.; Sun, J. ; Wang, Y. and Stoddart, J. F. 2016. Journal of the American Chemical Society 138, 11643-11653.

104. Mon, M.; Ferrando-Soria, J.; Grancha, T.; Fortea-Pérez, F. R.; Gascon, J. ; Leyva-Pérez, A.; Armentano, D. and Pardo, E. 2016. Journal of the American Chemical Society 138, 7864-7867.

105. Grant, R. A. and Drake, V. A. presented in part at the International Solvent Extraction Conference 2002, 2002.

106. Narita, H.; Tanaka, M.; Morisaku, K. and Abe, T. 2006. Hydrometallurgy 81, 153-158.

107. Mowafy, E. A. and Mohamed, D. 2016. Separation and Purification Technology 167, 146-153.

108. Preston, J. S. and du Preez, A. C. 1995. Solvent Extraction and Ion Exchange 13, 391-413.

109. Doidge, E. D.; Carson, I.; Tasker, P. A.; Ellis, R. J.; Morrison, C. A. and Love, J. B. 2016. Angewandte Chemie International Edition, 2016, 55, 12436-12439.

110. Ritcey, G.M. 1996. Solvent extraction processing plants, problems, assessments, solutions, Proc. ISEC'96, Australia.

111. Collet, S.; Chagnes, A.; Courtaud, B. ; Thiry, J.; Cote, G. 2009. Journal of Chemical Technology and Biotechnology 84 1331-1337.

112. Chagnes, A; Fossé, C.; Courtaud, B.; Thiry, J.; Cote, G. .2011. Hydrometallurgy 105 (3-4), 328-333.

113. Collet, S.; Chagnes, A.; Courtaud, B.; Thiry, J.; Cote, G. 2009. Journal of Chemical Technology and Biotechnology 84, 1331-1337.

114. Ciavatta, L.; Iuliano, M. 1995. Annali di chimica. 85, 235-255.

115. Markovic, M.; Pavkovic, N. 1983. Inorg. Chem. 22, 978-982.

116. Miguirditchian, M.; Bernier, G.; Pacary, V.; Balaguer, C.; Sorel, C.; Berlemont, R.; Fries, B.; Bertrand, M.; Cames, B.; Leydier, A.; Turgis, R.; Arrachart, G.; Pellet-Rostaing, S.; Mokhtari, H. 2016. Solvent Extraction and Ion Exchange 2016, 34.

117. Mokili, B.; Poitrenaud, C. 1996. Solvent Extraction and Ion Exchange 14, 617-634.

118. Mokili, B.; Poitrenaud, C. 1995. Solvent Extraction and Ion Exchange 13, 731-754.

119. Brønsted, J. N. 1922. J. Am. Chem. Soc. 44, 877-898.

120. Brønsted, J. N. 1922. J. Am. Chem. Soc. 1922, 44, 938-948

121. Sorel, C.; Montuir, M.; Balaguer, C.; Baron, P.; Dinh, B. The PAREX code: a powerful tool to model and simulate solvent extraction operations, Proceedings of the ISEC'11 conference, Santiago, Chile, 2011.

122. Iunga, B.; Levrat, E. Advanced Maintenance Services for Promoting Sustainability, Procedia CIRP 22 (2014) 15 – 22.

Figures

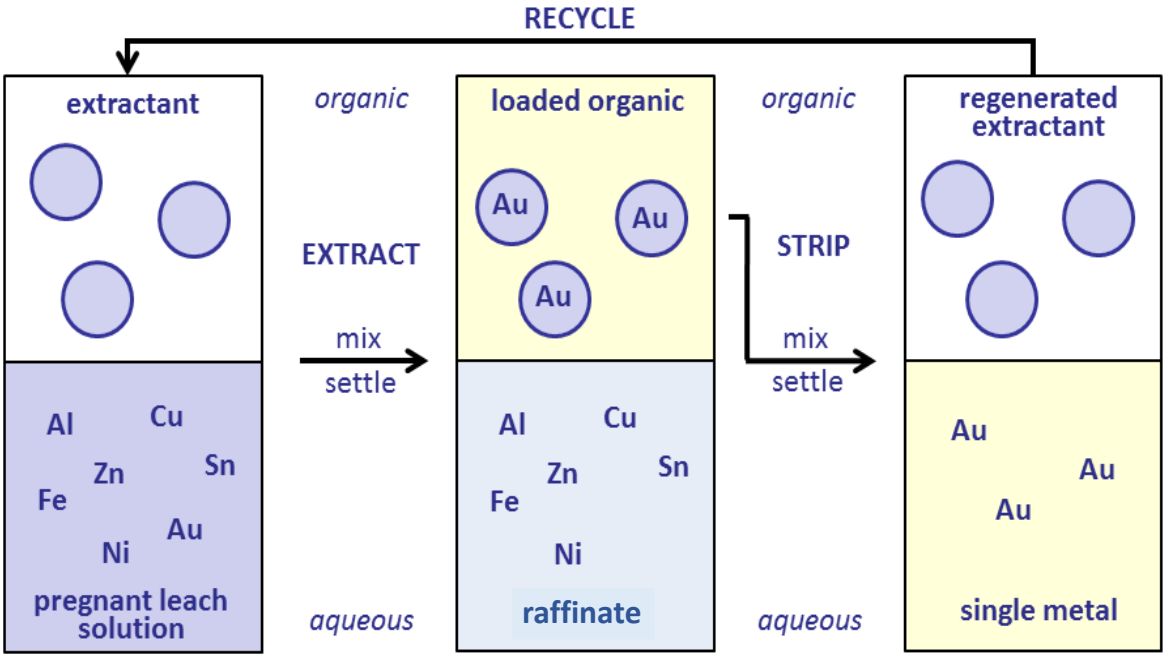

Figure 1 Schematic describing the separation of metals using solvent extraction. Circles in the organic phase represent extractant molecules or aggregates.

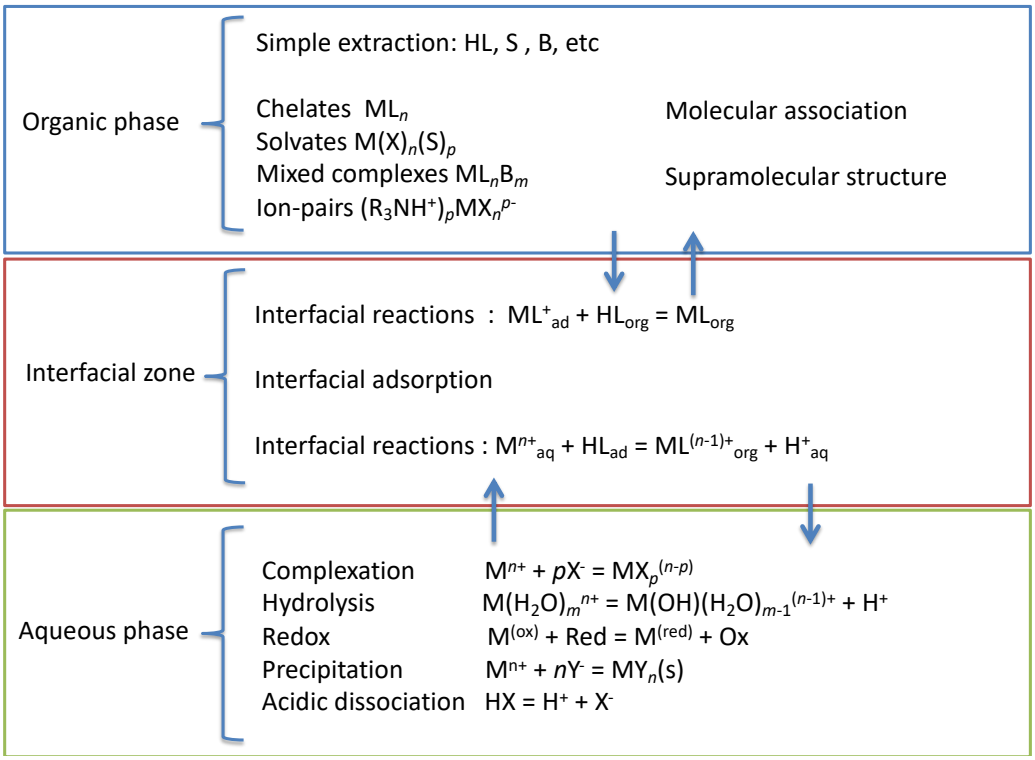

Figure 2 Main reactions involved in the liquid-liquid extractions of metals. Here, L is the conjugate anion of an acidic organic extractant, HL, often a chelant; B is a neutral

coordinating extractant; X is an anion co-extracted with the metal M from the aqueous phase.

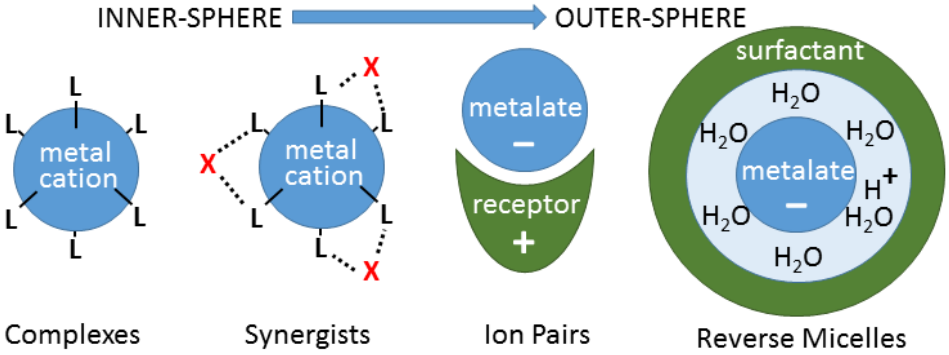

Figure 3 Modes of action generating charge-neutral assemblies in the water-immiscible phase in solvent extraction (L describes a neutral or anionic ligand).

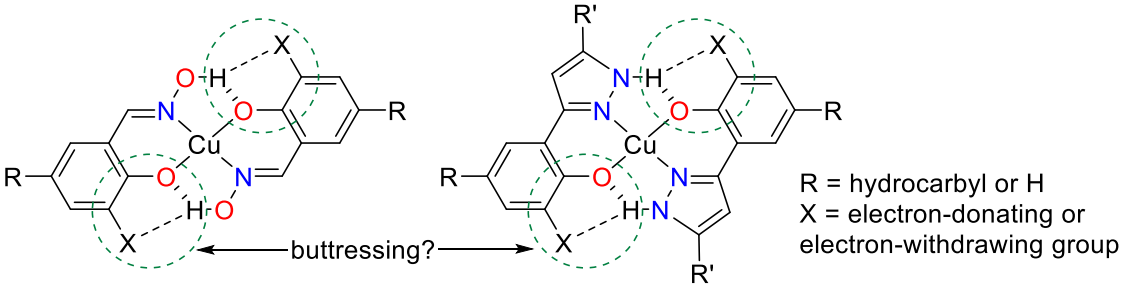

Figure 4 Buttressing of hydrogen-bonding interactions in *pseudo*-macrocyclic Cu complexes of phenolic aldoximes (left) and phenolic pyrazoles (right).

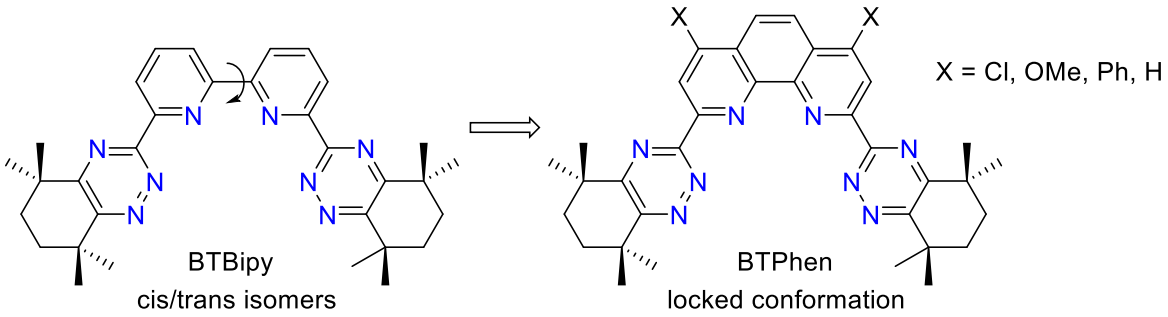

Figure 5 Triazinyl bipyridine and phenanthroline ligands for the separation of lanthanides from actinides.

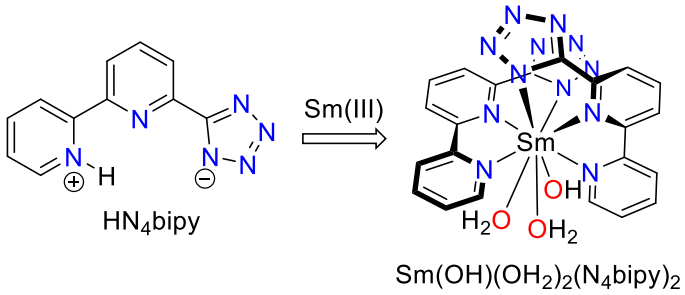

Figure 6 Coordination of the zwitterionic HN_4bipy to Sm(III) to form a 2:1 ligand:metal complex.

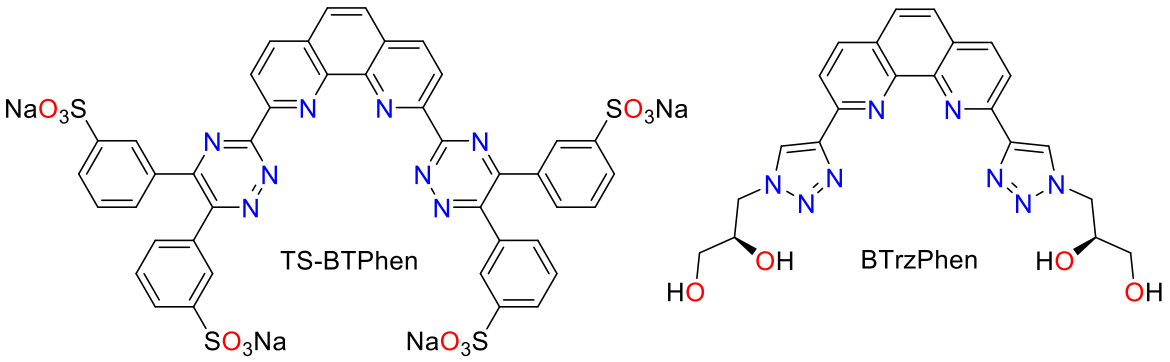

Figure 7 Hydrophilic ligands for the selective back-extraction of actinides into an aqueous phase.

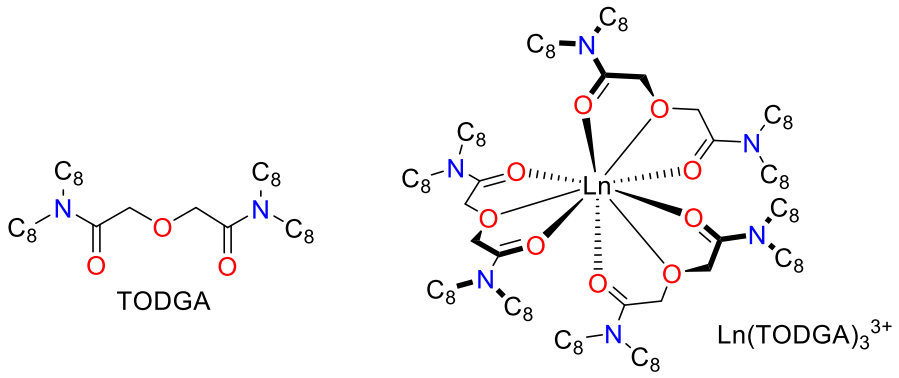

Figure 8 Lanthanide complexes of the diglycolamide TODGA.

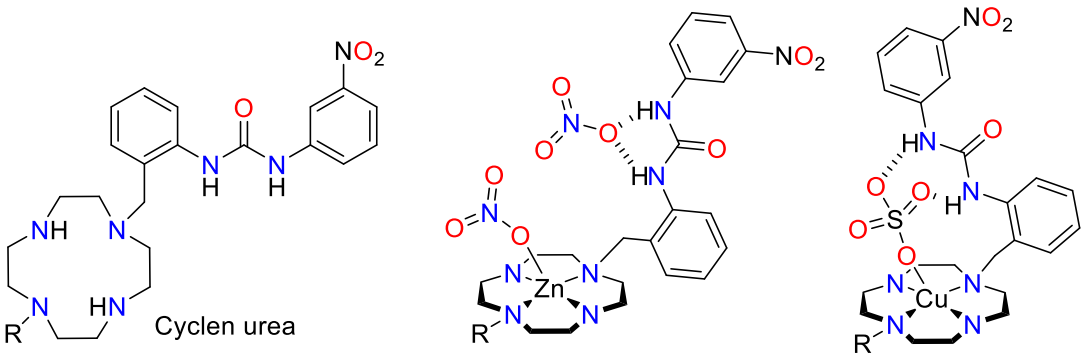

Figure 9 Ditopic ligands for simultaneous metal cation and anion binding.

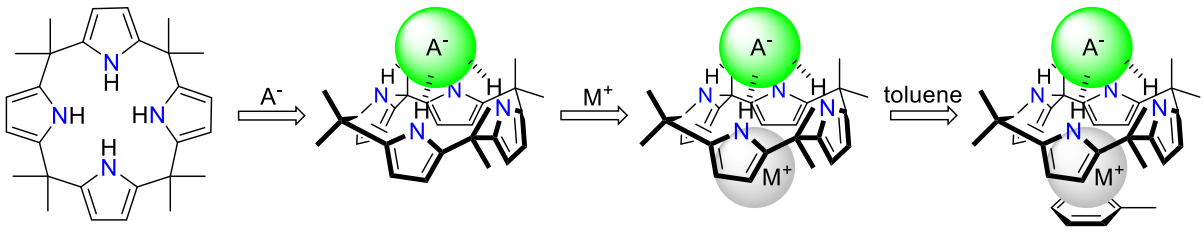

Figure 10 Calix[4]pyrroles as receptors for simple metal salts such as caesium halides.

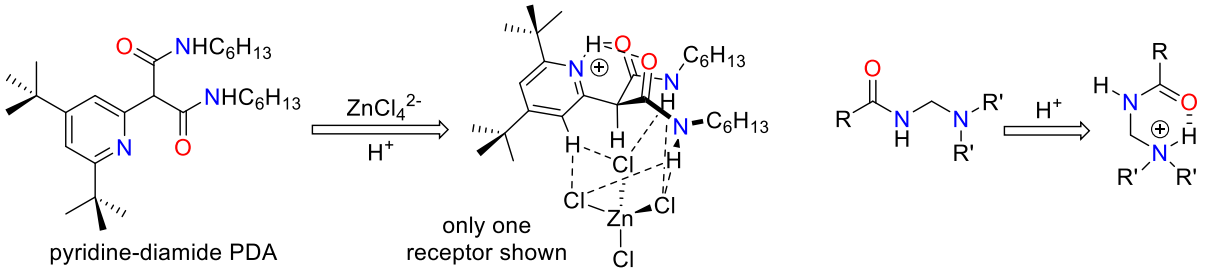

Figure 11 The formation of internal hydrogen bonds on protonation of a pyridine/amine-(di)amide resulting in receptors suited for metalate binding.

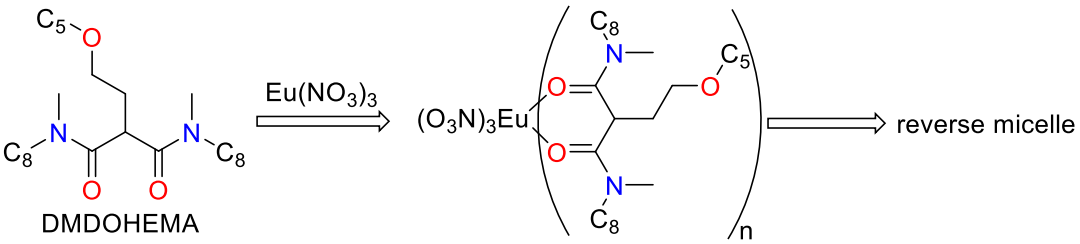

Figure 12 Sequential coordination and reverse micelle formation in the extraction of $Eu(NO_3)_3$ by a malonamide amphiphile.

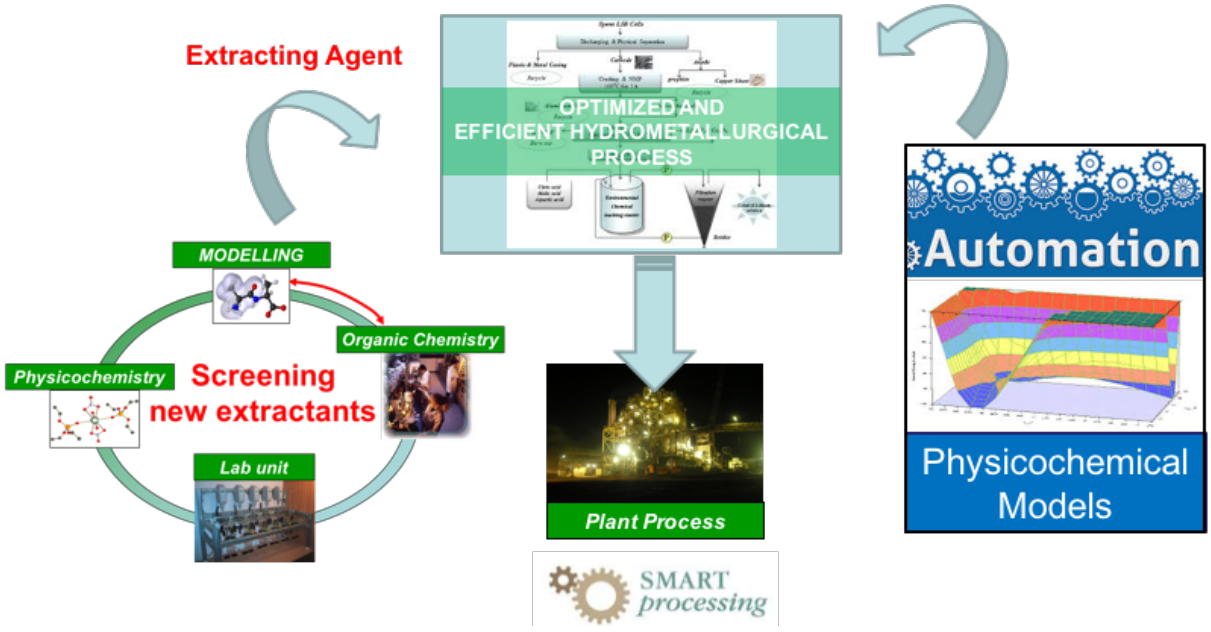

Figure 13 Smart processing approach.

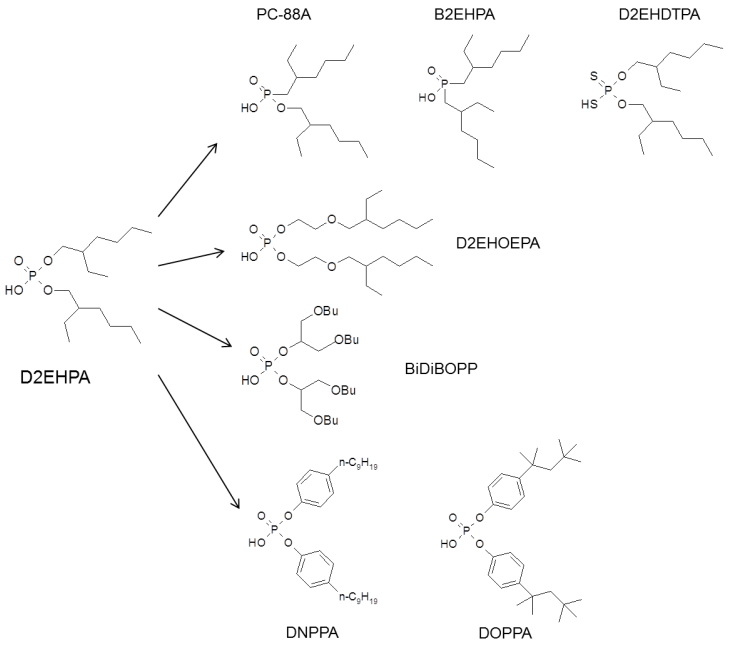

Figure 14 Molecular structure of different cationic exchangers tested in combination with TOPO for uranium extraction from WPA.

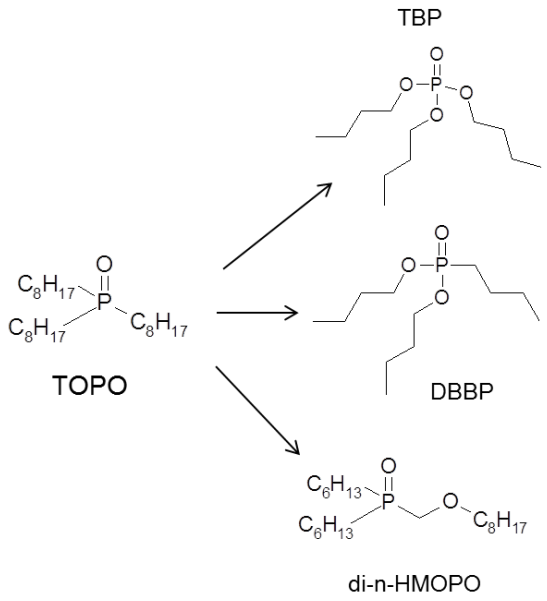

Figure 15 Molecular structure of different neutral-donor ligands tested in combination with D2EHPA for uranium extraction from WPA.

a) b)

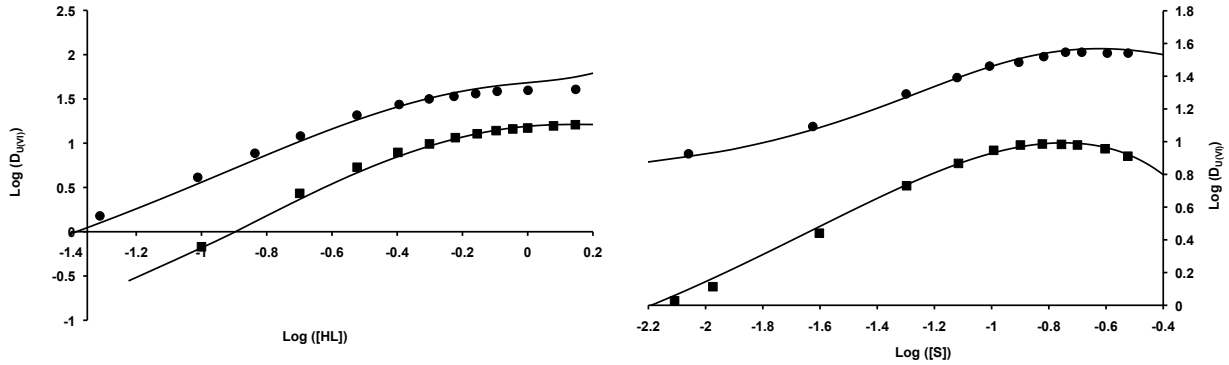

Figure 16 Logarithm of the distribution ratios of uranium(VI) between 5.3 M phosphoric acid and D2EHPA/TOPO (■) or BiDiBOPP/di-*n*-HMOPO (•) diluted in Isane IP 185 as a function of (a) the logarithm of initial D2EHPA or BiDiBOPP (HL) concentration at constant TOPO or di-*n*-HMOPO (S) concentration (0.125 M) and (b) the logarithm of initial TOPO or di-*n*-HMOPO concentration (S) at constant D2EHPA or BiDiBOPP (HL) concentration (0.5 M). Initial concentration of uranium = 1.43 10^{-3} M, temperature = (25.0 ± 0.2) °C, phase volume ratio V_o/V_a = 1. ——: Calculated with the thermodynamic model.

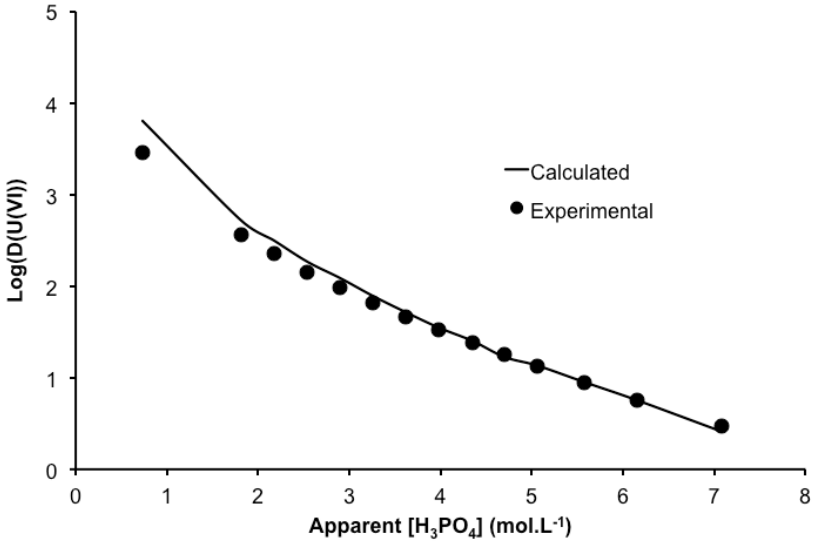

Figure 17 Experimental and calculated distribution ratios of uranium(VI) as a function of apparent concentration of phosphoric acid. Calculated line used the adjustable parameters of the thermodynamic model.

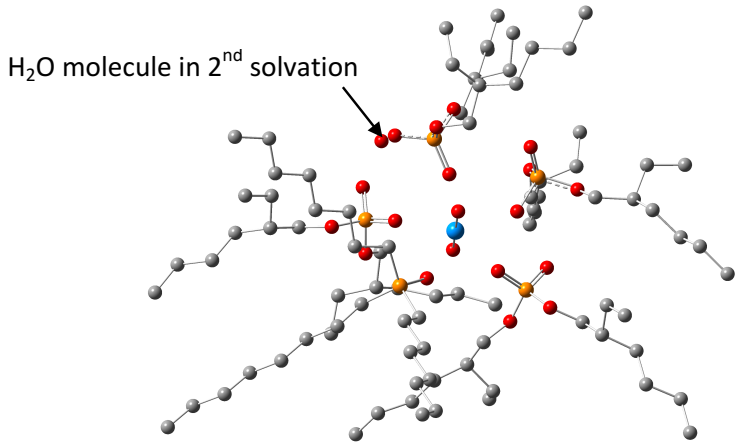

Figure 18 DFT calculation of the optimized geometry of $UO_2(HL)_2L_2(TOPO).H_2O$ (TOPO in the first solvation shell). Hydrogen atoms were removed from the figure for the sake of readability. Red atoms: oxygen. Orange atoms: phosphorus. Blue atoms: uranium. Gray atoms: carbon.

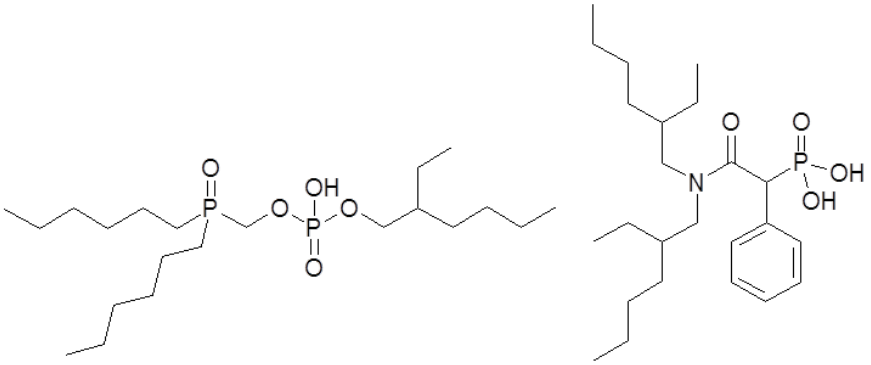

Figure 20 Molecular structures of *O*-methyldihexylphosphine oxide *O*-hexyl-2-ethyl phosphoric acid and *N*,*N*-di-2-ethylhexyl-carbamoylbenzylphosphonic acid.

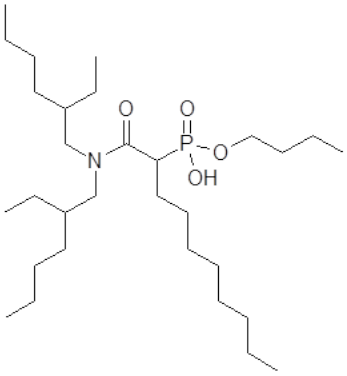

Figure 21 Molecular structure of butyl-1-[*N*,*N*-bis(2-ethylhexyl)carbamoylnonyl]phosphonic acid (DEHCNPB).

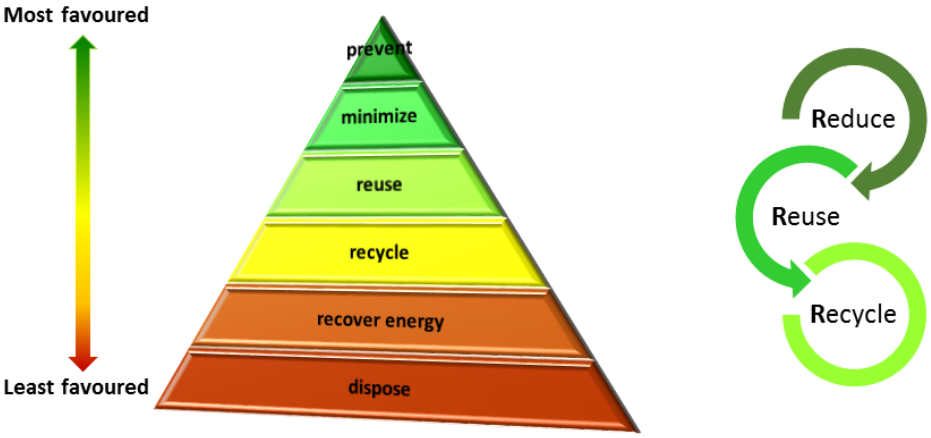

Figure 22 E-waste management hierarchy and 3R policy

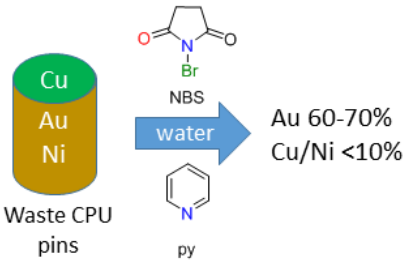

Figure 23 Selective leaching of gold using a synergistic mixture of NBS (70 mM) and py (100 mM) in water.

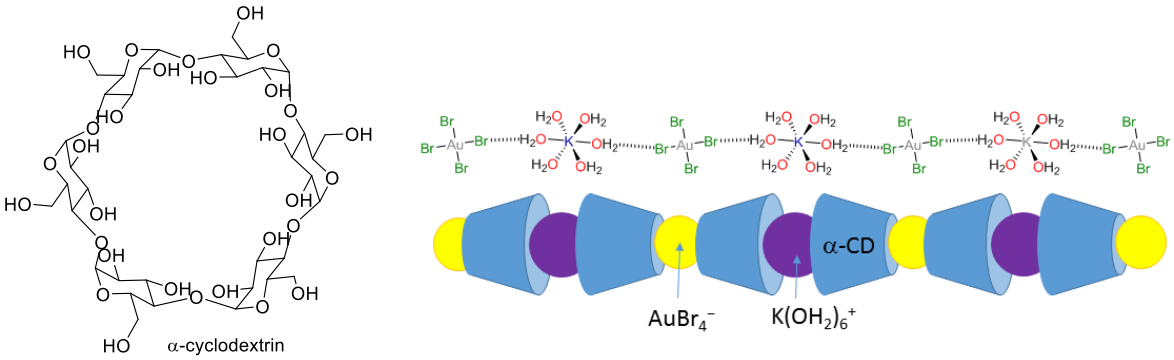

Figure 24 Spontaneous assembly of α-cyclodextrin (α-CD) with $KAuBr_4$ in water to form a one-dimensional extended-extended chain superstructure.

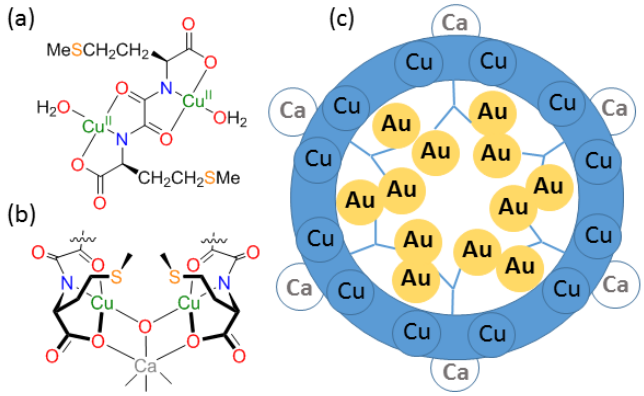

Figure 25 Methionine-decorated metal-organic frameworks for gold recovery: (a) dinuclear copper complex of the chiral bis(amino acid)oxalmide; (b) interaction of Ca^{2+} cations with dinuclear copper unit; (c) schematic of a single pore of the metal-organic framework structure in which the methionine groups coordinate to Au(I) centres within the pore.

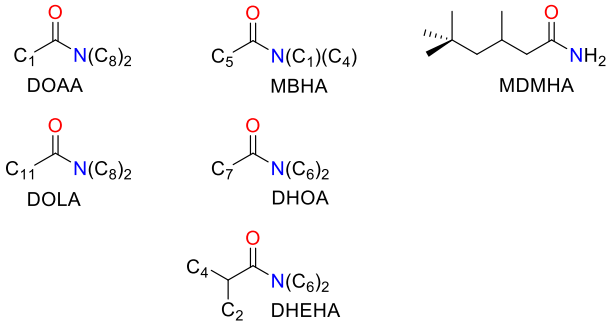

Figure 26 Tertiary and primary amides used in gold recovery by solvent extraction (C_n represents a straight-chain hydrocarbon substituent).

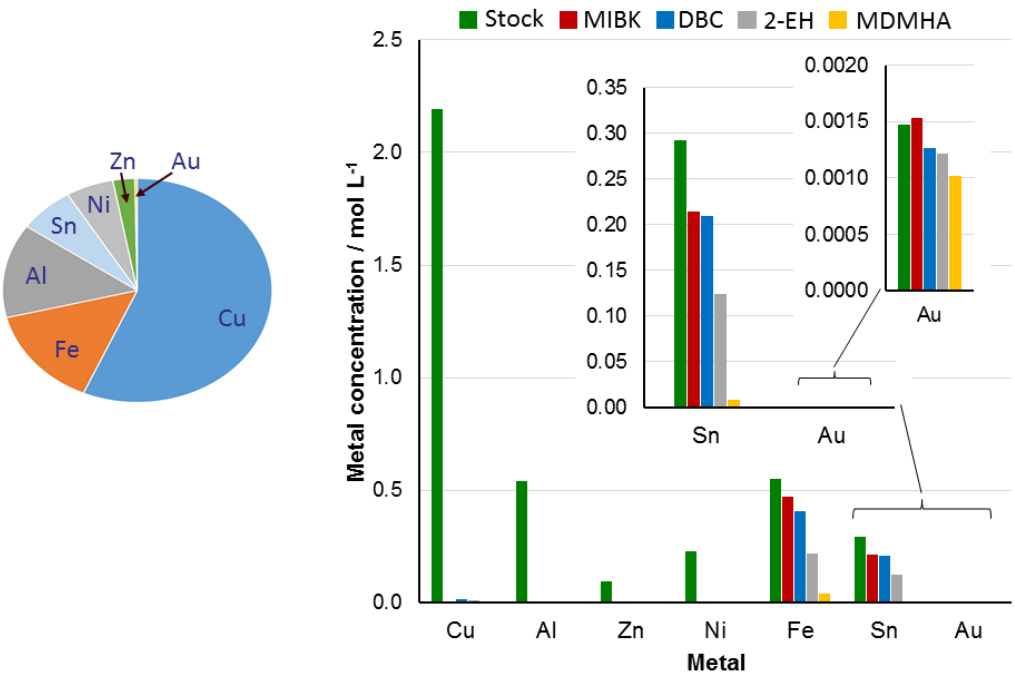

Figure 27 Left: Proportions of metals typically found in a smartphone device. Right: Comparison of the metals recovered by solvent extraction from a smartphone WEEE feed in 1.0 M HCl using the neat commercial reagents MIBK, DBC, and 2-EH and a 0.1 M toluene solution of the primary amide MDMHA.

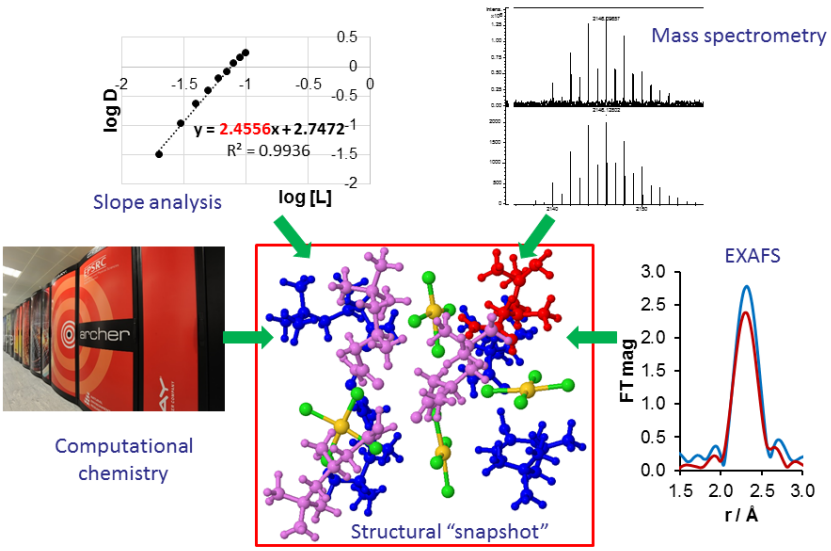

Figure 28 Combined analytical and spectroscopic techniques to determine the chemical speciation in the solvent extraction of gold from aqueous HCl using a toluene solution of MDMHA.

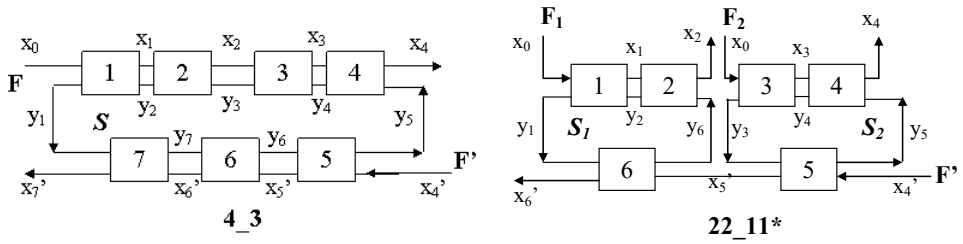

Figure 29 Classical countercurrent and unconventional two-feed flowsheets, 4_3 and 22_11*, respectively. x_i and y_i represent the metal concentration in the aqueous and organics phases of the mixer-settler *i*, respectively. S denotes the solvent flowrate, F, F1 and F2 are leach solution flowrates, respectively, and F' is the stripping flowrate. More information about the chemistry of uranium extraction by Alamine 336 is detailed in Refs 101-103.

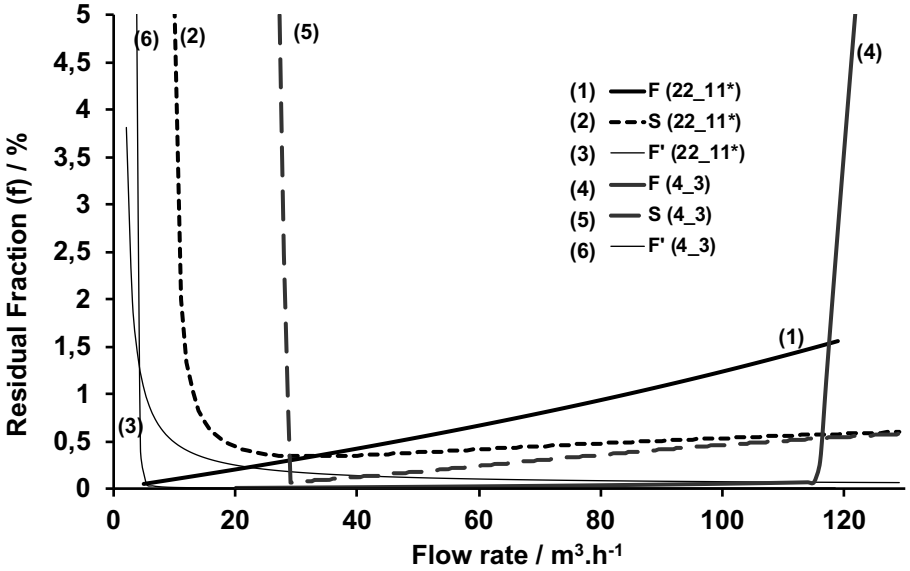

Figure 30 Influence of Solvent flow rate (*S*), feed flow rate (*F*) and stripping flow rate (*F'*) on the residual fraction (*f*) for the flowsheets 4_3 and 22_11*. The operating conditions for 4_3 and 22_11* are: S = 29 $m^3.h^{-1}$, F = 115 $m^3.h^{-1}$, F' = 4.8 $m^3.h^{-1}$, initial uranium concentration x_0 = 1677 $mg.L^{-1}$, and S = 29 $m^3.h^{-1}$, F = 90 $m^3.h^{-1}$, F' = 4.8 $m^3.h^{-1}$, initial uranium concentration x_0 = 400 $mg.L^{-1}$, respectively.

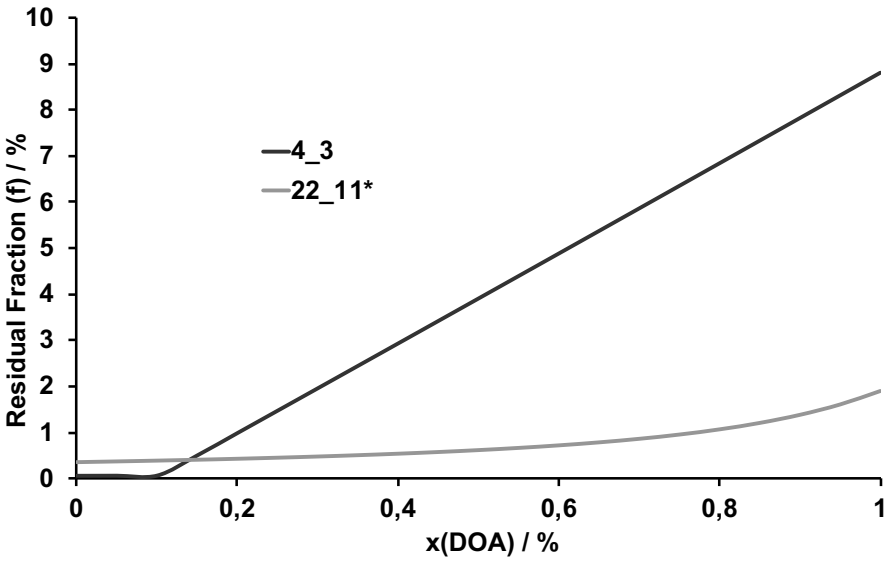

Figure 31 Influence of the dioctylamine molar fraction (*x*(DOA)) on the residual fraction (*f*) for the flowsheets 4_3 and 22_11*. The operating conditions for 4_3 and 22_11* are: solvent flow rate *S* = 29 $m^3.h^{-1}$, feed flow rate *F* = 115 $m^3.h^{-1}$, initial uranium concentration x_0 = 1677 $mg.L^{-1}$, and stripping flow rate *F'* = 4.80 $m^3.h^{-1}$, feed flow rate *F* = 90 $m^3.h^{-1}$, initial uranium concentration x_0 = 400 $mg.L^{-1}$, respectively.

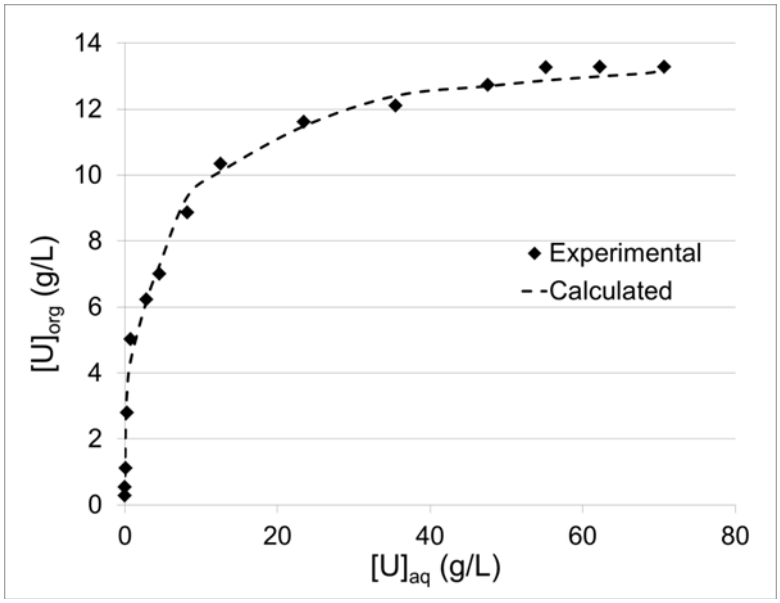

Figure 32 Comparison of experimental and calculated isotherms of uranium(VI) extraction with 0.1 M DEHCNPB/TPH and 5 M H_3PO_4.

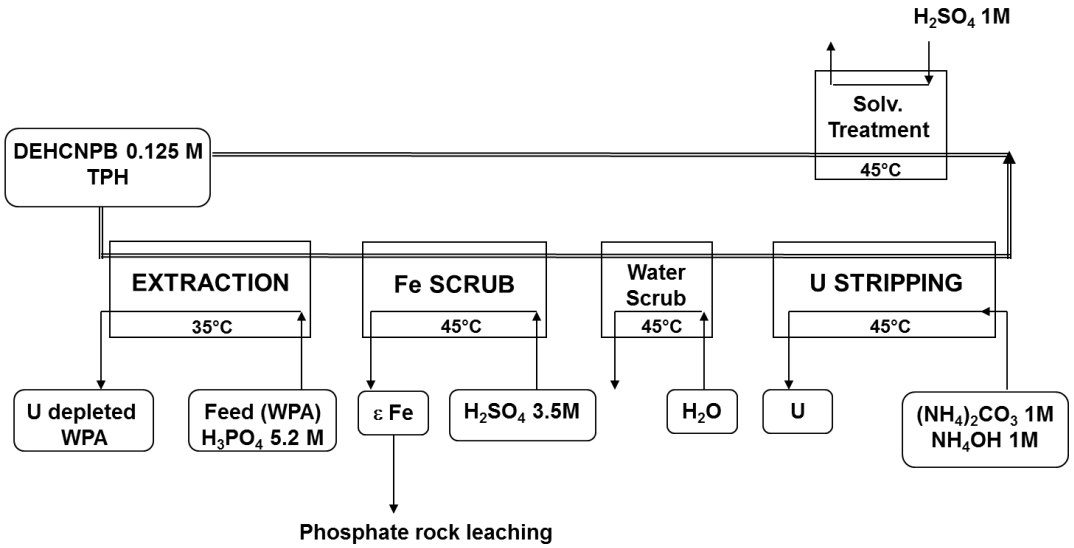

Figure 33 Flowsheet of the continuous test performed in mixer-settlers with DEHCNPB.

Table

Table 1 Equilibria considered in aqueous phase to calculate uranium(VI) and iron(III) speciation in phosphoric acid

Equilibrium	log(β) at I = 0 and 25 °C
$H_3PO_4 \leftrightharpoons H_2PO_4^- + H^+$	–2.14
$H_2PO_4^- \leftrightharpoons HPO_4^{2-} + H^+$	–7.21
$HPO_4^{2-} \leftrightharpoons PO_4^{3-} + H^+$	–12.35
$UO_2^{2+} + H_3PO_4 \leftrightharpoons UO_2(H_2PO_4)^+ + H^+$	1.5
$UO_2^{2+} + H_3PO_4 \leftrightharpoons UO_2(H_3PO_4)^{2+}$	1.3
$UO_2^{2+} + 2\,H_3PO_4 \leftrightharpoons UO_2(H_2PO_4)_2 + 2\,H^+$	1.3
$UO_2^{2+} + 2\,H_3PO_4 \leftrightharpoons UO_2\left(H_2PO_4\right)(H_3PO_4)^+ + H^+$	2.3
$Fe^{3+} + 2\,H_2PO_4^- + H_3PO_4 \leftrightharpoons FeH(H_2PO_4)_3^+$	8.3
$Fe^{3+} + 3\,H_2PO_4^- \leftrightharpoons Fe(H_2PO_4)_3$	9.8